Options Pricing under Shared-jump Diffusion Model by Fourier Space Time-stepping Method

by

Bangyao Xu

A thesis
presented to the University of Waterloo
in fulfillment of the
thesis requirement for the degree of
Master of Mathematics
in
Computational Mathematics

Supervisors: Prof. Peter Forsyth & Prof. George Labahn

Waterloo, Ontario, Canada, 2018

I hereby declare that I am the sole author of this thesis. This is a true copy of the thesis, including any required final revisions, as accepted by my examiners.

I understand that my thesis may be made electronically available to the public.

Abstract

In this essay, a shared-jump diffusion model is introduced to describe financial shocks and contagion effects. Under the shared-jump diffusion model for underlying assets, the derivation of the Fourier Space Time-stepping (FST) method is demonstrated to solve the corresponding partial integro-differential equations (PIDE). Numerical results of pricing single- and multi-asset European options under three kinds of jump diffusion models are presented. In addition, constant padding is proposed to reduce the wrap-around error in one- and two-dimensional cases. The data from global financial markets in recent decades are used to conduct the empirical analysis.

Acknowledgements

I would like to thank my supervisors, Professor Peter Forsyth and Professor George Labahn, for their guidance, support and encouragement throughout this year.

Also, I want to express my sincere thanks to Professor Yuying Li, for reading this eassy and providing valuable suggestions.

To my parents, for their love and inspiration throughout my life.

To my dear friends, for always sharing ideas and making progress with me: Ershi, Xukun, Wenqing, Kasun, Boon, Jessie, Fan, Linqi, Edward and Emily.

Last but not least, I want to thank our director, Dr. Jeff Orchard and coordinator, Amanda Guderian, for their information and suggestion on daily life.

Dedication

This is dedicated to Cheryl, the one I love.

Table of Contents

List of Tables

List of Figures

Chapter 1

Introduction

In finance, a derivative is a contract between two or more parties whose value is based on a particular underlying asset or a basket of underlying assets. The most common underlying instruments include bonds, commodities, currencies, interest rates, market indices and stocks. Some of the more common derivatives include forwards, futures, options, swaps, and variations such as synthetic collateralized debt obligations (CDOs) and credit default swaps (CDSs).

Derivatives are mainly used for speculating and purpose of risk management. By holding derivatives, speculators take risks to pursue potential quick, large profits. Meanwhile, investors can effectively hedge various risks through the use of derivatives. That is, derivatives offer market participants the chance to customize satisfactory risk profiles for their own businesses.

An option is a contract which gives the buyer the right, but not the obligation, to buy or sell an underlying asset at a specified strike price, on or before expiration. A European option can only be exercised on expiration while an American option can be exercised on any trading day before expiry.

To price derivatives, the assumption of a stochastic process model for the underlying asset is required. The well-known Black-Scholes model was first proposed by Black and Scholes (1973)[3]. In this model, the underlying asset price is assumed to follow a geometric Brownian motion and the no-arbitrage price of options can be determined as the solution of a partial differential equation (PDE). The jump diffusion model was first suggested by Merton (1976)[14]. A Poisson-driven random jump component is added to geometric Brownian motion in order to represent the abnormal changes in underlying price. When the underlying asset follows a jump diffusion model, the pricing problem reduces to solving a partial integro-differential equation (PIDE).

The Fourier Space Time-stepping (FST) method was first developed by Jackson, Jaimungal and Surkov (2008)[8]. FST method uses the Fourier transform to solve the PDE or PIDE numerically. The continuous Fourier transform (CFT) is a linear operator which maps spatial derivatives into multiplications in Fourier space. Because of the convenient properties of the Fourier transform, the PDE or PIDE in real space can be converted into a linear first-order ordinary differential equation (ODE) in Fourier space, which can be easily solved in closed-form. In practice, the discrete Fourier transform (DFT) is used to approximate the CFT so the continuous domain is discretized for computational purpose. Unfortunately, the FST method causes wrap-around error in the option value solution, which needs to be addressed.

With the development of economic globalization, contagion effects tend to be inevitable as the result of financial shocks. The contagion literature identifies at least three possible mechanisms by which shocks in one market may spill over into other markets. First, Allen and Gale (2000)[1] suggested that contagion occurs through a liquidity shock across all markets. Second, Kiyotaki and Moore (2002)[9] claimed that contagion can be viewed as the transmission of information from more-liquid markets or markets with more rapid price discovery to other markets. Third, Vayanos (2004)[18] concluded that contagion occurs as negative returns in the distressed market affect subsequent returns in other markets via a time-varying risk premium.

Besides the theoretical research on financial contagion, plenty of empirical tests are conducted as well. By constructing a set of dummy variables using daily news to capture the impact of own-country and cross-border news on the markets, Baig and Goldfajn (1999)[2] found that correlations in currency and sovereign spreads between the financial markets of Thailand, Malaysia, Indonesia, Korea, and the Philippines increased significantly during the Asian crisis period. Longstaff (2010)[12] found strong evidence of contagion in the financial markets by investigating the pricing of subprime asset-backed collateralized debt obligations (CDOs) and their contagion effects on other markets.

In this essay, a shared-jump diffusion model is introduced with the motivation of describing financial shocks and contagion effects. Under this model, two underlying assets are assumed to go through abnormal changes at the same time. In other words, two underlying assets share the same jump driven by unique Poisson process. The FST method is implemented to solve the corresponding PIDE under the shared-jump diffusion model. Also, constant padding is developed to remedy the wrap-around error in one- and two-dimensional cases. Last but not least, empirical data analysis is carried out to estimate the parameters and provide evidence for developing the shared-jump diffusion model.

The remainder of this essay is structured as follows. Chapter 2 introduces one-factor jump diffusion model, two-factor jump diffusion model and the new shared-jump diffusion model. Chapter 3 presents the derivation of the Fourier Space Time-stepping (FST) method under shared-jump diffusion model. Chapter 4 provides numerical examples under various models and the appropriate treatment of wrap-around error. Chapter 5 gives the empirical analysis based on the real data from global financial markets. Chapter 6 lists the conclusions. The Appendix provides the Fourier transform of distributions, the FST algorithms for European options and methodology of Monte Carlo simulation.

Chapter 2

Mathematical Models

2.1 Introduction

The Black-Scholes-Merton (BSM) model for pricing of options, assumes the prices of underlying assets follow geometric Brownian motion. By assuming certain ideal conditions on financial markets and constructing a self-financing replicating portfolio, Black and Scholes (1973)[3] show that the option pricing problem under the BSM model can be reduced to solving a second-order partial differential equation (PDE).

In order to take random jumps into consideration, Merton (1976)[14] suggested a jump diffusion model to describe the dramatic changes in underlying prices within a very short time period. That model adds a Poisson process, which may cause discontinuities in sample paths, to the geometric Brownian motion. The distribution of random jump sizes are commonly chosen to follow a log-normal distribution or a double exponential distribution by Kou (2002)[10]. Under the jump diffusion model, as with the BSM model, the option pricing problem reduces to solving a second-order partial integro-differential equation (PIDE).

In this chapter, a new two-asset jump diffusion model is introduced to capture the extreme cases which happened in global financial markets such as the dot-com bubble[1] in 2002 and the financial crisis[2] in 2008. Under the shared-jump diffusion model, the

[1] A historic economic bubble and period of excessive speculation that occurred roughly from 1997 to 2001, a period of extreme growth in the usage and adaptation of the Internet.

[2] A crisis first started in the subprime mortgage market in the United States, and then developed into a full-blown international banking crisis.

random jumps and their jump sizes are driven by the single Poisson process, which is quite reasonable to characterize the financial shocks and the corresponding contagion effects on global markets.

2.2 One-factor Jump Diffusion Model

The sample paths of the underlying price S are modelled by a stochastic differential equation:

$$\frac{dS}{S} = \mu dt + \sigma dZ + (\eta - 1)dq, \tag{2.1}$$

where

$$\begin{aligned}
\mu &= \text{drift rate,} \\
\sigma &= \text{underlying volatility,} \\
dZ &= \text{increment of standard Brownian motion,} \\
\eta - 1 &= \text{impulse function producing a jump from } S \text{ to } S\eta, \\
dq &= \begin{cases} 0, & \text{with probability } 1 - \lambda dt, \\ 1, & \text{with probability } \lambda dt, \end{cases} \\
\lambda &= \text{mean arrival rate of Poisson jump.}
\end{aligned}$$

Let $\mathcal{V}(S, \tau)$ be the option value, with $\tau = T - t$, the time to expiry T. By Ito's Lemma and no-arbitrage arguments, a partial integro-differential equation (PIDE)for $\mathcal{V}(S, \tau)$[15, 19] can be written as:

$$\mathcal{V}_\tau = \frac{\sigma^2 S^2}{2}\mathcal{V}_{SS} + (r - \lambda\kappa)S\mathcal{V}_S - (r + \lambda)\mathcal{V} + \left(\lambda \int_0^\infty \mathcal{V}(S\eta)g(\eta)d\eta\right) \tag{2.2}$$

where

$$\begin{aligned}
T &= \text{expiry time,} \\
r &= \text{risk free rate,} \\
\tau &= T - t, \text{where } t \text{ is current time,} \\
\kappa &= E[\eta - 1], \text{where } E[\eta] = \int_0^\infty \eta g(\eta)d\eta, \\
g(\eta) &= \text{probability density function of the jump magnitude}
\end{aligned}$$

with the initial condition:

$$\mathcal{V}(S,0) = \max(S-K,0), \quad \text{for call option} \tag{2.3}$$

or

$$\mathcal{V}(S,0) = \max(K-S,0), \quad \text{for put option} \tag{2.4}$$

where K is the strike price. Here, introduce $f(x) = g(e^x)e^x$ as the density function of $\log(\eta)$. So, with Merton jump density (normal distribution), we have

$$f(y) = \frac{1}{\sqrt{2\pi}\gamma} e^{-\frac{1}{2}(\frac{y-\mu}{\gamma})^2},$$

where μ and γ are constant parameters. Using the Kou jump density (double exponential distribution), we get

$$f(y) = p\eta_1 e^{-y\eta_1} \cdot 1_{\{y\geq 0\}} + (1-p)\eta_2 e^{y\eta_2} \cdot 1_{\{y\leq 0\}},$$

where p is the probability of an upward jump and η_1, η_2 are constant parameters.

2.3 Two-factor Jump Diffusion Model

Intuitively, it is easy to extend single-asset cases to multi-asset cases. For example, in two dimensions, by introducing the correlation coefficient between the Brownian motions of two different underlying prices, the stochastic differential equations for the underlying prices S_1, S_2 can be written as:

$$\frac{dS_1}{S_1} = \mu_1 dt + \sigma_1 dZ_1 + (\eta_1 - 1)dq_1, \tag{2.5}$$

$$\frac{dS_2}{S_2} = \mu_2 dt + \sigma_2 dZ_2 + (\eta_2 - 1)dq_2, \tag{2.6}$$

$$dZ_1 dZ_2 = \rho dt \tag{2.7}$$

where

$$
\begin{aligned}
\mu_1, \mu_2 &= \text{drift rates,}\\
\sigma_1, \sigma_2 &= \text{underlying volatilities,}\\
dZ_1, dZ_2 &= \text{increments of standard Brownian motions,}\\
\eta_1 - 1, \eta_2 - 1 &= \text{impulse functions producing jumps from } (S_1, S_2) \text{ to } (S_1\eta_1, S_2\eta_2),\\
dq_1 &= \begin{cases} 0, & \text{with probability } 1 - \lambda_1 dt,\\ 1, & \text{with probability } \lambda_1 dt,\end{cases}\\
dq_2 &= \begin{cases} 0, & \text{with probability } 1 - \lambda_2 dt,\\ 1, & \text{with probability } \lambda_2 dt,\end{cases}\\
\lambda_1, \lambda_2 &= \text{mean arrival rates of Poisson jumps,}\\
\rho &= \text{correlation of two standard Brownian motions.}
\end{aligned}
$$

Define $\mathcal{V}(S_1, S_2, \tau)$ as the two-asset option value. As before, the partial integro-differential equation (PIDE) for $\mathcal{V}(S_1, S_2, \tau)$ can be obtained by Ito's Lemma and no-arbitrage arguments as:

$$
\begin{aligned}
\mathcal{V}_\tau =& \frac{\sigma_1^2 S_1^2}{2}\mathcal{V}_{S_1S_1} + \frac{\sigma_2^2 S_2^2}{2}\mathcal{V}_{S_2S_2} + (r - \lambda_1\kappa_1)S_1\mathcal{V}_{S_1} + (r - \lambda_2\kappa_2)S_2\mathcal{V}_{S_2} + \rho\sigma_1\sigma_2 S_1 S_2 \mathcal{V}_{S_1S_2}\\
&- (r + \lambda_1 + \lambda_2)\mathcal{V} + \left(\lambda_1 \int_0^\infty \mathcal{V}(S_1\eta_1) g(\eta_1) d\eta_1\right) + \left(\lambda_2 \int_0^\infty \mathcal{V}(S_2\eta_2) g(\eta_2) d\eta_2\right)
\end{aligned}
\tag{2.8}
$$

where

$$
\begin{aligned}
T &= \text{expiry time,}\\
r &= \text{risk free rate,}\\
\tau &= T - t, \text{where } t \text{ is current time,}\\
\kappa_1 &= E[\eta_1 - 1], \text{where } E[\eta_1] = \int_0^\infty \eta_1 g(\eta_1) d\eta_1,\\
\kappa_2 &= E[\eta_2 - 1], \text{where } E[\eta_2] = \int_0^\infty \eta_2 g(\eta_2) d\eta_2,\\
g(\eta_1) &= \text{probability density function of the jump magnitude of } S_1,\\
g(\eta_2) &= \text{probability density function of the jump magnitude of } S_2.
\end{aligned}
$$

Examples of the initial conditions include:

$$\mathcal{V}(S_1, S_2, 0) = \max(B_2S_2 - B_1S_1 - K, 0), \quad \text{for spread call option} \tag{2.9}$$

or

$$\mathcal{V}(S_1, S_2, 0) = \max(K - B_2S_2 + B_1S_1, 0), \quad \text{for spread put option} \tag{2.10}$$

or

$$\mathcal{V}(S_1, S_2, 0) = \max(S_1 - K_1, K_2 - S_2, 0), \quad \text{for dual strike option} \tag{2.11}$$

where K, K_1, K_2, B_1 and B_2 are parameters for various multi-asset options.

2.4 Shared-jump Diffusion Model

Slightly different from equations (2.5) and (2.6), the shared-jump here is driven by a single Poisson process. Assume two underlying assets S_1, S_2 follow the stochastic differential equations:

$$\frac{dS_1}{S_1} = \mu_1 dt + \sigma_1 dZ_1 + (\eta - 1)dq, \tag{2.12}$$

$$\frac{dS_2}{S_2} = \mu_2 dt + \sigma_2 dZ_2 + (\eta - 1)dq, \tag{2.13}$$

$$dZ_1 dZ_2 = \rho dt \tag{2.14}$$

where

$$dq = \begin{cases} 0, & \text{with probability } 1 - \lambda dt, \\ 1, & \text{with probability } \lambda dt, \end{cases}$$

$$\begin{aligned} \mu_1, \mu_2 &= \text{drift rates,} \\ \sigma_1, \sigma_2 &= \text{underlying volatilities,} \\ dZ_1, dZ_2 &= \text{increments of standard Brownian motions,} \\ \eta - 1 &= \text{impulse function producing the shared-jump from } (S_1, S_2) \text{ to } (S_1\eta, S_2\eta), \\ \lambda &= \text{mean arrival rate of Poisson jump,} \\ \rho &= \text{correlation of two standard Brownian motions.} \end{aligned}$$

Let $\mathcal{V}(S_1, S_2, t)$ be the two-asset option value under the shared-jump diffusion model. The partial integro-differential equation (PIDE) for $\mathcal{V}(S_1, S_2, t)$ can be derived by Ito's Lemma and constructing a hedging portfolio.

By Ito's Lemma for jump processes, the total variation of $\mathcal{V}(S_1, S_2, t)$ can be written as:

$$\begin{aligned} d\mathcal{V} = & \mathcal{V}_t dt + \mathcal{V}_{S_1}(\mu_1 S_1 dt + \sigma_1 S_1 dZ_1) + \mathcal{V}_{S_2}(\mu_2 S_2 dt + \sigma_2 S_2 dZ_2) + \mathcal{V}_{S_1 S_2}\rho\sigma_1\sigma_2 S_1 S_2 dt \\ & + \frac{1}{2}\mathcal{V}_{S_1 S_1}\sigma_1^2 S_1^2 dt + \frac{1}{2}\mathcal{V}_{S_2 S_2}\sigma_2^2 S_2^2 dt + [\mathcal{V}(S_1\eta, S_2\eta, t) - \mathcal{V}(S_1, S_2, t)]dq, \end{aligned} \tag{2.15}$$

in more compact notation, we have:

$$\begin{aligned} d\mathcal{V} = & \ \alpha\ dt + \beta\ dZ_1 + \gamma\ dZ_2 + \Delta\mathcal{V}\ dq, \\ & \alpha = \mathcal{V}_t + \mathcal{V}_{S_1}\mu_1 S_1 + \mathcal{V}_{S_2}\mu_2 S_2 \\ & \quad + \frac{1}{2}\mathcal{V}_{S_1 S_1}\sigma_1^2 S_1^2 + \frac{1}{2}\mathcal{V}_{S_2 S_2}\sigma_2^2 S_2^2 + \mathcal{V}_{S_1 S_2}\rho\sigma_1\sigma_2 S_1 S_2, \\ & \beta = \mathcal{V}_{S_1}\sigma_1 S_1, \\ & \gamma = \mathcal{V}_{S_2}\sigma_2 S_2, \\ & \Delta\mathcal{V} = [\mathcal{V}(S_1\eta, S_2\eta, t) - \mathcal{V}(S_1, S_2, t)]. \end{aligned}$$

Consider the portfolio Π including four contracts $\mathcal{V}_1, \mathcal{V}_2, \mathcal{V}_3$ and $\mathcal{V}_4$ such that

$$\Pi = n_1\mathcal{V}_1 + n_2\mathcal{V}_2 + n_3\mathcal{V}_3 + n_4\mathcal{V}_4. \tag{2.16}$$

Hence,

$$\begin{aligned} d\Pi &= n_1 d\mathcal{V}_1 + n_2 d\mathcal{V}_2 + n_3 d\mathcal{V}_3 + n_4 d\mathcal{V}_4 \\ &= n_1(\alpha_1\ dt + \beta_1\ dZ_1 + \gamma_1\ dZ_2 + \Delta\mathcal{V}_1\ dq) \\ &\quad + n_2(\alpha_2\ dt + \beta_2\ dZ_1 + \gamma_2\ dZ_2 + \Delta\mathcal{V}_2\ dq) \\ &\quad + n_3(\alpha_3\ dt + \beta_3\ dZ_1 + \gamma_3\ dZ_2 + \Delta\mathcal{V}_3\ dq) \\ &\quad + n_4(\alpha_4\ dt + \beta_4\ dZ_1 + \gamma_4\ dZ_2 + \Delta\mathcal{V}_4\ dq) \\ &= (n_1\alpha_1 + n_2\alpha_2 + n_3\alpha_3 + n_4\alpha_4)\ dt \\ &\quad + (n_1\beta_1 + n_2\beta_2 + n_3\beta_3 + n_4\beta_4)\ dZ_1 \\ &\quad + (n_1\gamma_1 + n_2\gamma_2 + n_3\gamma_3 + n_4\gamma_4)\ dZ_2 \\ &\quad + (n_1\Delta\mathcal{V}_1 + n_2\Delta\mathcal{V}_2 + n_3\Delta\mathcal{V}_3 + n_4\Delta\mathcal{V}_4)\ dq. \end{aligned} \tag{2.17}$$

Eliminate the random terms dZ_1, dZ_2 and dq by setting

$$\begin{aligned} n_1\beta_1 + n_2\beta_2 + n_3\beta_3 + n_4\beta_4 &= 0, \\ n_1\gamma_1 + n_2\gamma_2 + n_3\gamma_3 + n_4\gamma_4 &= 0, \\ n_1\Delta\mathcal{V}_1 + n_2\Delta\mathcal{V}_2 + n_3\Delta\mathcal{V}_3 + n_4\Delta\mathcal{V}_4 &= 0. \end{aligned} \tag{2.18}$$

Thus, the portfolio Π is risk-less. Let r be the risk free rate, so that

$$d\Pi = r\Pi \; dt. \tag{2.19}$$

From equations (2.17), (2.18) and (2.19), we get:

$$(n_1\alpha_1 + n_2\alpha_2 + n_3\alpha_3 + n_4\alpha_4) = (n_1\mathcal{V}_1 + n_2\mathcal{V}_2 + n_3\mathcal{V}_3 + n_4\mathcal{V}_4)r. \tag{2.20}$$

Putting equations (2.18) and (2.20) together gives

$$\begin{bmatrix} \beta_1 & \beta_2 & \beta_3 & \beta_4 \\ \gamma_1 & \gamma_2 & \gamma_3 & \gamma_4 \\ \Delta\mathcal{V}_1 & \Delta\mathcal{V}_2 & \Delta\mathcal{V}_3 & \Delta\mathcal{V}_4 \\ \alpha_1 - r\mathcal{V}_1 & \alpha_2 - r\mathcal{V}_2 & \alpha_3 - r\mathcal{V}_3 & \alpha_4 - r\mathcal{V}_4 \end{bmatrix} \begin{bmatrix} n_1 \\ n_2 \\ n_3 \\ n_4 \end{bmatrix} = \begin{bmatrix} 0 \\ 0 \\ 0 \\ 0 \end{bmatrix}. \tag{2.21}$$

Equation (2.21) has a non-zero solution only if the rows are linearly dependent. So, there must exist $\lambda_{B_1}(S_1, S_2, t), \lambda_{B_2}(S_1, S_2, t)$ and $\lambda_J(S_1, S_2, t)$ such that

$$\begin{aligned} (\alpha_1 - r\mathcal{V}_1) &= \lambda_{B_1}\beta_1 + \lambda_{B_2}\gamma_1 - \lambda_J\Delta\mathcal{V}_1, \\ (\alpha_2 - r\mathcal{V}_2) &= \lambda_{B_1}\beta_2 + \lambda_{B_2}\gamma_2 - \lambda_J\Delta\mathcal{V}_2, \\ (\alpha_3 - r\mathcal{V}_3) &= \lambda_{B_1}\beta_3 + \lambda_{B_2}\gamma_3 - \lambda_J\Delta\mathcal{V}_3, \\ (\alpha_4 - r\mathcal{V}_4) &= \lambda_{B_1}\beta_4 + \lambda_{B_2}\gamma_4 - \lambda_J\Delta\mathcal{V}_4. \end{aligned}$$

It can be shown that $\lambda_J \geq 0$ avoids any arbitrage opportunity. Dropping the subscripts gives

$$(\alpha - r\mathcal{V}) = \lambda_{B_1}\beta + \lambda_{B_2}\gamma - \lambda_J\Delta\mathcal{V} \tag{2.22}$$

and substituting α, β, γ and $\Delta\mathcal{V}$ leads to

$$\begin{aligned} &\mathcal{V}_t + (\mu_1 - \lambda_{B_1}\sigma_1)\mathcal{V}_{S_1}S_1 + (\mu_2 - \lambda_{B_2}\sigma_2)\mathcal{V}_{S_2}S_2 + \mathcal{V}_{S_1S_2}\rho\sigma_1\sigma_2S_1S_2 \\ &\quad + \frac{1}{2}\mathcal{V}_{S_1S_1}\sigma_1^2S_1^2 + \frac{1}{2}\mathcal{V}_{S_2S_2}\sigma_2^2S_2^2 - r\mathcal{V} + \lambda_J[\mathcal{V}(S_1\eta, S_2\eta, t) - \mathcal{V}(S_1, S_2, t)] = 0. \end{aligned} \tag{2.23}$$

Suppose $\mathcal{V}_3 = S_1$ and $\mathcal{V}_4 = S_2$ are two traded underlying assets. In this case, we have:

$$\begin{aligned} \alpha_3 &= \mu_1S_1, & \alpha_4 &= \mu_2S_2, \\ \beta_3 &= \sigma_1S_1, & \beta_4 &= 0, \\ \gamma_3 &= 0, & \gamma_4 &= \sigma_2S_2, \\ \Delta\mathcal{V}_3 &= (\eta - 1)S_1, & \Delta\mathcal{V}_4 &= (\eta - 1)S_2. \end{aligned}$$

From equation (2.22), we get:

$$
\begin{aligned}
(\mu_1 S_1 - rS_1) &= \lambda_{B_1}\sigma_1 S_1 + \lambda_{B_2}(0) - \lambda_J(\eta-1)S_1, \\
(\mu_2 S_2 - rS_2) &= \lambda_{B_1}(0) + \lambda_{B_2}\sigma_2 S_2 - \lambda_J(\eta-1)S_2.
\end{aligned} \tag{2.24}
$$

After eliminating common factors in equation (2.24), it is easy to obtain:

$$
\begin{aligned}
\mu_1 - \lambda_{B_1}\sigma_1 &= r - \lambda_J(\eta-1), \\
\mu_2 - \lambda_{B_2}\sigma_2 &= r - \lambda_J(\eta-1).
\end{aligned} \tag{2.25}
$$

Substituting equation (2.25) into equation (2.23) gives

$$
\begin{aligned}
&\mathcal{V}_t + [r - \lambda_J(\eta-1)]\mathcal{V}_{S_1}S_1 + [r - \lambda_J(\eta-1)]\mathcal{V}_{S_2}S_2 + \mathcal{V}_{S_1S_2}\rho\sigma_1\sigma_2 S_1 S_2 \\
&\quad + \frac{1}{2}\mathcal{V}_{S_1S_1}\sigma_1^2 S_1^2 + \frac{1}{2}\mathcal{V}_{S_2S_2}\sigma_2^2 S_2^2 - r\mathcal{V} + \lambda_J[\mathcal{V}(S_1\eta, S_2\eta, t) - \mathcal{V}(S_1, S_2, t)] = 0.
\end{aligned} \tag{2.26}
$$

Assume the number of jump states is finite, which means the asset price S may jump to any states $S\eta_i$ after a jump where $i = 1, \cdots, n$. By the hedging arguments above, use $n+3$ hedging instruments so that the diffusion and jumps will be hedged perfectly. Then equation (2.23) can be written as:

$$
\begin{aligned}
&\mathcal{V}_t + (\mu_1 - \lambda_{B_1}\sigma_1)\mathcal{V}_{S_1}S_1 + (\mu_2 - \lambda_{B_2}\sigma_2)\mathcal{V}_{S_2}S_2 + \mathcal{V}_{S_1S_2}\rho\sigma_1\sigma_2 S_1 S_2 \\
&\quad + \frac{1}{2}\mathcal{V}_{S_1S_1}\sigma_1^2 S_1^2 + \frac{1}{2}\mathcal{V}_{S_2S_2}\sigma_2^2 S_2^2 - r\mathcal{V} + \sum_{i=1}^{n}\lambda_J^i[\mathcal{V}(S_1\eta_i, S_2\eta_i, t) - \mathcal{V}(S_1, S_2, t)] = 0.
\end{aligned} \tag{2.27}
$$

Similarly, if the underlying assets can also be used for hedging, equation (2.26) can be transformed into:

$$
\begin{aligned}
&\mathcal{V}_t + [r - \sum_{i=1}^{n}\lambda_J^i(\eta_i-1)]\mathcal{V}_{S_1}S_1 + [r - \sum_{i=1}^{n}\lambda_J^i(\eta_i-1)]\mathcal{V}_{S_2}S_2 + \mathcal{V}_{S_1S_2}\rho\sigma_1\sigma_2 S_1 S_2 \\
&\quad + \frac{1}{2}\mathcal{V}_{S_1S_1}\sigma_1^2 S_1^2 + \frac{1}{2}\mathcal{V}_{S_2S_2}\sigma_2^2 S_2^2 - r\mathcal{V} + \sum_{i=1}^{n}\lambda_J^i[\mathcal{V}(S_1\eta_i, S_2\eta_i, t) - \mathcal{V}(S_1, S_2, t)] = 0.
\end{aligned} \tag{2.28}
$$

Let $g(\eta_i) = \frac{\lambda_J^i}{\sum_{i=1}^n \lambda_J^i}$ and $\lambda = \sum_{i=1}^n \lambda_J^i$, then equation (2.27) becomes:

$$
\begin{aligned}
&\mathcal{V}_t + (\mu_1 - \lambda_{B_1}\sigma_1)\mathcal{V}_{S_1}S_1 + (\mu_2 - \lambda_{B_2}\sigma_2)\mathcal{V}_{S_2}S_2 + \mathcal{V}_{S_1S_2}\rho\sigma_1\sigma_2 S_1 S_2 \\
&\quad + \frac{1}{2}\mathcal{V}_{S_1S_1}\sigma_1^2 S_1^2 + \frac{1}{2}\mathcal{V}_{S_2S_2}\sigma_2^2 S_2^2 - r\mathcal{V} + \lambda\sum_{i=1}^{n} g(\eta_i)[\mathcal{V}(S_1\eta, S_2\eta, t) - \mathcal{V}(S_1, S_2, t)] = 0.
\end{aligned} \tag{2.29}
$$

In addition, $g(\eta_i) \geq 0$ and $\lambda \geq 0$ because $\lambda_J^i \geq 0$.

Now, if we take the limit as the number of jump states goes to infinity, then $g(\eta)$ will tend to a continuous distribution and infinite hedging instruments are required. Thus, equation (2.29) can be represented as:

$$\begin{aligned}
&\mathcal{V}_t + (\mu_1 - \lambda_{B_1}\sigma_1)\mathcal{V}_{S_1}S_1 + (\mu_2 - \lambda_{B_2}\sigma_2)\mathcal{V}_{S_2}S_2 + \mathcal{V}_{S_1S_2}\rho\sigma_1\sigma_2 S_1 S_2 \\
&\quad + \frac{1}{2}\mathcal{V}_{S_1S_1}\sigma_1^2 S_1^2 + \frac{1}{2}\mathcal{V}_{S_2S_2}\sigma_2^2 S_2^2 - r\mathcal{V} + \lambda\int_0^\infty [\mathcal{V}(S_1\eta, S_2\eta, t) - \mathcal{V}(S_1, S_2, t)]g(\eta)d\eta = 0.
\end{aligned} \tag{2.30}$$

In the case where the underlying assets can be used to hedge the risk, we have:

$$\begin{aligned}
&\mathcal{V}_t + (r - \lambda E[\eta - 1])\mathcal{V}_{S_1}S_1 + (r - \lambda E[\eta - 1])\mathcal{V}_{S_2}S_2 + \mathcal{V}_{S_1S_2}\rho\sigma_1\sigma_2 S_1 S_2 \\
&\quad + \frac{1}{2}\mathcal{V}_{S_1S_1}\sigma_1^2 S_1^2 + \frac{1}{2}\mathcal{V}_{S_2S_2}\sigma_2^2 S_2^2 - r\mathcal{V} + \lambda\int_0^\infty [\mathcal{V}(S_1\eta, S_2\eta, t) - \mathcal{V}(S_1, S_2, t)]g(\eta)d\eta = 0.
\end{aligned} \tag{2.31}$$

It is crucial to point out that λ and $g(\eta)$ here are not the real mean arrival rate of Poisson jump and real probability density function of the jump magnitude because they are obtained by the hedging arguments mentioned above. Thus, λ and $g(\eta)$ must be derived by calibration to the financial market data.

Define $\tau = T - t$ and $\kappa = E[\eta - 1] = \int_0^\infty (\eta - 1)g(\eta)d\eta$, the partial integro-differential equation (PIDE) for $\mathcal{V}(S_1, S_2, \tau)$ can be directly derived from equations (2.31):

$$\begin{aligned}
\mathcal{V}_\tau =& \frac{1}{2}\sigma_1^2 S_1^2 \mathcal{V}_{S_1S_1} + \frac{1}{2}\sigma_2^2 S_2^2 \mathcal{V}_{S_2S_2} + (r - \lambda\kappa)S_1\mathcal{V}_{S_1} + (r - \lambda\kappa)S_2\mathcal{V}_{S_2} \\
&+ \rho\sigma_1\sigma_2 S_1 S_2 \mathcal{V}_{S_1S_2} - (r + \lambda)\mathcal{V} + \lambda\int_0^\infty \mathcal{V}(S_1\eta, S_2\eta)g(\eta)d\eta
\end{aligned} \tag{2.32}$$

with the initial condition given by equation (2.9), (2.10) or (2.11).

A log-transformation will lead to a PIDE with constant coefficients and a cross-correlation integral. Define $x_1 = \log(S_1), x_2 = \log(S_2)$ and let $v(x_1, x_2, \tau) = \mathcal{V}(S_1, S_2, \tau)$. The relationships between the partial derivatives of v with respect to x_1, x_2 and partial derivatives of V with respect to S_1, S_2 can be seen as:

$$\mathcal{V}_{S_1} = \frac{v_{x_1}}{e^{x_1}}, \quad \mathcal{V}_{S_2} = \frac{v_{x_2}}{e^{x_2}},$$

$$\mathcal{V}_{S_1S_1} = \frac{v_{x_1x_1} - v_{x_1}}{e^{2x_1}}, \quad \mathcal{V}_{S_2S_2} = \frac{v_{x_2x_2} - v_{x_2}}{e^{2x_2}}, \quad \mathcal{V}_{S_1S_2} = \frac{v_{x_1x_2}}{e^{x_1}e^{x_2}}.$$

Let $\eta = e^y$, then $d\eta = e^y dy$. Plugging the above into equation (2.32) gives the PIDE in terms of v:

$$
\begin{aligned}
v_\tau =& \frac{1}{2}\sigma_1^2 v_{x_1x_1} + \frac{1}{2}\sigma_2^2 v_{x_2x_2} + (r - \lambda\kappa - \frac{1}{2}\sigma_1^2)v_{x_1} + (r - \lambda\kappa - \frac{1}{2}\sigma_2^2)v_{x_2} \\
&+ \rho\sigma_1\sigma_2 v_{x_1x_2} - (r+\lambda)v + \lambda\Big(\int_{-\infty}^{\infty} v(x_1 + y, x_2 + y, \tau)g(e^y)e^y dy\Big).
\end{aligned}
\tag{2.33}
$$

Introducing $f(x) = g(e^x)e^x$ and substituting into the PIDE (2.33) gives:

$$
\begin{aligned}
v_\tau =& \frac{1}{2}\sigma_1^2 v_{x_1x_1} + \frac{1}{2}\sigma_2^2 v_{x_2x_2} + (r - \lambda\kappa - \frac{1}{2}\sigma_1^2)v_{x_1} + (r - \lambda\kappa - \frac{1}{2}\sigma_2^2)v_{x_2} \\
&+ \rho\sigma_1\sigma_2 v_{x_1x_2} - (r+\lambda)v + \lambda\Big(\int_{-\infty}^{\infty} v(x_1 + y, x_2 + y, \tau)f(y)dy\Big).
\end{aligned}
\tag{2.34}
$$

Hence, with log-transformation and changes of variables, the original PIDE (2.32) may be represented as the PIDE (2.34), which contains constant coefficients and a cross-correlation integral.

Chapter 3

Fourier Space Time-stepping Method

3.1 Introduction

The Fourier space time-stepping (FST) method was first developed by Jackson, Jaimungal and Surkov (2008)[8]. This method uses the continuous Fourier transform, which is a linear operator, to map the spatial derivatives into multiplications in Fourier space.

By the properties of the Fourier transform, the PIDE derived previously in (2.23) can be converted into a linear first-order ordinary differential equation (ODE) in Fourier space. This is then straightforward to solve in closed-form.

For one-factor and two-factor jump diffusion models, the details of implementing the FST method are demonstrated by Lippa (2013)[11]. In this chapter, the FST algorithm under a shared-jump diffusion model will be discussed.

3.2 Continuous Fourier Transform

The continuous Fourier transform (CFT) maps a function in the space domain $f(\mathbf{x})$ into a function in the frequency domain $F(\mathbf{k})$. Here, $\mathbf{x}$ and $\mathbf{k}$ can be scalars or vectors since it is straightforward to generalize a one-dimensional continuous Fourier transform into higher dimensions.

With the definition of one-dimensional continuous Fourier transform of a function $f(x)$ being:

$$F(k) = \mathcal{F}[f(x)](k) := \int_{-\infty}^{\infty} f(x)e^{-i2\pi kx}dx, \tag{3.1}$$

the definition of one-dimensional inverse continuous Fourier transform (ICFT) of a function $F(k)$ is:

$$f(x) = \mathcal{F}^{-1}[F(k)](x) := \int_{-\infty}^{\infty} F(k)e^{i2\pi kx}dk. \tag{3.2}$$

With the definition of two-dimensional continuous Fourier transform of a function $f(x)$ being :

$$F(k_1, k_2) = \mathcal{F}[f(x_1, x_2)](k_1, k_2) := \int_{-\infty}^{\infty}\int_{-\infty}^{\infty} f(x_1, x_2)e^{-i2\pi(k_1x_1+k_2x_2)}dx_1dx_2, \tag{3.3}$$

the definition of two-dimensional inverse continuous Fourier transform of a function $F(k)$ is:

$$f(x_1, x_2) = \mathcal{F}^{-1}[F(k_1, k_2)](x_1, x_2) := \int_{-\infty}^{\infty}\int_{-\infty}^{\infty} F(k_1, k_2)e^{i2\pi(k_1x_1+k_2x_2)}dk_1dk_2. \tag{3.4}$$

There are some useful properties of Fourier transform for computations. The Fourier transform of the partial derivative of a function $v(x, \tau)$ with respect to τ can be represented as:

$$\mathcal{F}\big[\frac{\partial}{\partial\tau}v(x, \tau)\big](k) = \frac{\partial}{\partial\tau}\mathcal{F}[v(x, \tau)](k). \tag{3.5}$$

Also, the Fourier transform of the partial derivative of a function $v(x, \tau)$ with respect to x can be represented as:

$$\mathcal{F}\big[\frac{\partial^n}{\partial x^n}v(x, \tau)\big](k) = (2\pi ik)^n\mathcal{F}[v(x, \tau)](k). \tag{3.6}$$

In addition, the two-dimensional Fourier transform of the the second partial derivative of a function $v(x, y, \tau)$ with respect to x and y can be represented as:

$$\mathcal{F}\big[\frac{\partial^2}{\partial x\partial y}v(x, y, \tau)\big](k_1, k_2) = (2\pi ik_1)(2\pi ik_2)\mathcal{F}[v(x, y, \tau)](k_1, k_2). \tag{3.7}$$

3.3 Discrete Fourier Transform

Generally, it is impossible to compute the exact result of continuous Fourier transform in closed-form. So, the discrete Fourier transform (DFT) is introduced to approximate CFT for numerical solutions. This has error $\mathcal{O}(\Delta x^2)$, where Δx is the constant spacing in the x direction. In the following, we define the DFT pairs as:

$$\hat{F}_n = \sum_{m=0}^{N-1} f(x_m) e^{-i2\pi\frac{nm}{N}},$$
$$f_m = \frac{1}{N} \sum_{n=-\frac{N}{2}+1}^{\frac{N}{2}} e^{i2\pi\frac{nm}{N}} \hat{F}_n.$$

If the original domain of $[-\infty, \infty]$ is truncated to the new domain $\Omega = [x_{min}, x_{max}]$, the continuous Fourier transform (3.1) is approximated on domain Ω as:

$$F(k) \approx \int_{x_{min}}^{x_{max}} f(x) e^{-i2\pi kx} dx. \tag{3.8}$$

Discretizing the real domain $[x_{min}, x_{max}]$ as:

$$x_m = x_{min} + m \cdot \Delta x \tag{3.9}$$

where $m = 0, 1, \cdots, N-1, \Delta x = \frac{x_{max}-x_{min}}{N}$ and N is the total number of nodes in the real domain.

Meanwhile, the Fourier domain can also be discretized as:

$$k_n = \frac{n}{x_{max} - x_{min}} \tag{3.10}$$

where $n = -\frac{N}{2} + 1, \cdots, \frac{N}{2}$. By the Nyquist frequency conditions, the maximum frequency is $\pm\frac{N}{2}$. Therefore, the allowable frequencies are:

$$\Big\{\big(-\frac{N}{2}+1\big), \cdots, \frac{N}{2}\Big\}. \tag{3.11}$$

We can approximate this using the trapezoidal rule, so equation (3.8) becomes:

$$\begin{aligned} F(k) &\approx \int_{x_{min}}^{x_{max}} f(x) e^{-i2\pi kx} dx \\ &\approx \sum_{m=0}^{N-1} f(x_m) e^{-i2\pi k x_m} \Delta x + \mathcal{O}(\Delta x^2). \end{aligned} \tag{3.12}$$

In Fourier space, for $k_{-\frac{N}{2}+1}, \cdots, k_{\frac{N}{2}}$, we use equations (3.10) and (3.12) to get:

$$\begin{aligned} F_n = F(k_n) &\approx \sum_{m=0}^{N-1} f(x_m) e^{-i2\pi k_n x_m} \Delta x \\ &= \Delta x \sum_{m=0}^{N-1} f(x_m) e^{-i2\pi k_n (x_{min} + m\Delta x)} \\ &= e^{-i2\pi k_n x_{min}} \Delta x \sum_{m=0}^{N-1} f(x_m) e^{-i2\pi \frac{nm}{N}}. \end{aligned} \tag{3.13}$$

Define $\hat{F}_n := \sum_{m=0}^{N-1} f(x_m) e^{-i2\pi \frac{nm}{N}}$. Then, equation (3.13) can be rewritten as:

$$F_n = e^{-i2\pi k_n x_{min}} \cdot \Delta x \cdot \hat{F}_n \tag{3.14}$$

where $\hat{F}_0, \hat{F}_1, \cdots, \hat{F}_{N-1}$ are the discrete Fourier transforms of $f_0, f_1, \cdots, f_{N-1}$.

Conversely, the inverse continuous Fourier transform (3.2) can be approximated by:

$$\begin{aligned} f(x) &= \int_{-\infty}^{\infty} F(k) e^{i2\pi kx} dk \\ &\approx \int_{-\frac{N}{2}}^{\frac{N}{2}} F(k) e^{i2\pi kx} dk \\ &\approx \sum_{n=-\frac{N}{2}+1}^{\frac{N}{2}} F(k_n) e^{i2\pi k_n x} \Delta k + \mathcal{O}(\Delta k^2) \end{aligned} \tag{3.15}$$

where $k_n = n \cdot \Delta k$ and $\Delta k = \frac{1}{x_{max} - x_{min}}$.

In this situation:

$$
\begin{aligned}
f_m = f(x_m) &\approx \sum_{n=-\frac{N}{2}+1}^{\frac{N}{2}} F(k_n) e^{i2\pi k_n x_m} \Delta k \\
&= \sum_{n=-\frac{N}{2}+1}^{\frac{N}{2}} F(k_n) e^{i2\pi k_n (x_{min}+m\Delta x)} \Delta k \\
&= \sum_{n=-\frac{N}{2}+1}^{\frac{N}{2}} \big(e^{-i2\pi k_n x_{min}} \cdot \Delta x \cdot \hat{F}_n\big) e^{i2\pi k_n (x_{min}+m\Delta x)} \Delta k \\
&= \sum_{n=-\frac{N}{2}+1}^{\frac{N}{2}} \Delta x \cdot e^{i2\pi \frac{nm}{N}} \hat{F}_n \cdot \Delta k \\
&= \frac{1}{N} \sum_{n=-\frac{N}{2}+1}^{\frac{N}{2}} e^{i2\pi \frac{nm}{N}} \hat{F}_n
\end{aligned}
\tag{3.16}
$$

where $f_0, f_1, \cdots, f_{N-1}$ are the inverse discrete Fourier transforms (IDFT) of $\hat{F}_0, \hat{F}_1, \cdots, \hat{F}_{N-1}$.

3.4 FST Method under a Shared-jump Diffusion Model

3.4.1 Fourier Transform

Given a partial integro-differential differential equation in the form of equation (2.23), with constant coefficients and a cross-correlation integral term, the option pricing problem can be reduced to solving the PIDE by the Fourier space time-stepping method. Applying the two-dimensional continuous Fourier transform $\mathcal{F}$ on the PIDE (2.23) gives:

$$
\begin{aligned}
\mathcal{F}[v_\tau](k_1,k_2) =& \frac{1}{2}\sigma_1^2 \mathcal{F}[v_{x_1x_1}](k_1,k_2) + \frac{1}{2}\sigma_2^2 \mathcal{F}[v_{x_2x_2}](k_1,k_2) \\
&+ (r-\lambda\kappa-\frac{1}{2}\sigma_1^2)\mathcal{F}[v_{x_1}](k_1,k_2) + (r-\lambda\kappa-\frac{1}{2}\sigma_2^2)\mathcal{F}[v_{x_2}](k_1,k_2) \\
&+ \rho\sigma_1\sigma_2 \mathcal{F}[v_{x_1x_2}](k_1,k_2) - (r+\lambda)\mathcal{F}[v](k_1,k_2) \\
&+ \lambda \mathcal{F}\big[\int_{-\infty}^{\infty} v(x_1+y, x_2+y) f(y) dy\big](k_1,k_2)
\end{aligned}
\tag{3.17}
$$

where the transform variables k_1, k_2 represent the frequencies.

In equation (3.17), except for the two-dimensional cross-correlation integral term, all other terms can be easily simplified by properties (3.5), (3.6) and (3.7). Take the two-dimensional Fourier transform of cross-correlation integral term to get:

$$\begin{aligned}&\mathcal{F}\Big[\int_{-\infty}^{\infty} v(x_1+y, x_2+y)f(y)dy\Big](k_1,k_2)\\ &=\int_{-\infty}^{\infty}\int_{-\infty}^{\infty}\Big(\int_{-\infty}^{\infty} v(x_1+y,x_2+y)f(y)dy\Big)e^{-2\pi i(k_1x_1+k_2x_2)}dx_1dx_2.\end{aligned} \tag{3.18}$$

Let $w=-y$, so that $dy=-dw$. Plugging into (3.18) gives:

$$\begin{aligned}&\mathcal{F}\Big[\int_{-\infty}^{\infty} v(x_1+y, x_2+y)f(y)dy\Big](k_1,k_2)\\ &=\int_{-\infty}^{\infty} f(-w)\Big(\int_{-\infty}^{\infty}\int_{-\infty}^{\infty} v(x_1-w,x_2-w)e^{-2\pi i(k_1x_1+k_2x_2)}dx_1dx_2\Big)dw.\end{aligned} \tag{3.19}$$

Let $u_1=x_1-w, u_2=x_2-w$, so that $du_1=dx_1, du_2=dx_2$. Plugging into (3.19) gives:

$$\begin{aligned}&\mathcal{F}\Big[\int_{-\infty}^{\infty} v(x_1+y, x_2+y)f(y)dy\Big](k_1,k_2)\\ &=\int_{-\infty}^{\infty} f(-w)\Big[\int_{-\infty}^{\infty}\int_{-\infty}^{\infty} v(u_1,u_2)e^{-2\pi i(k_1(u_1+w)+k_2(u_2+w))}du_1du_2\Big]dw\\ &=\int_{-\infty}^{\infty} e^{-2\pi i(k_1+k_2)w}f(-w)dw\int_{-\infty}^{\infty}\int_{-\infty}^{\infty} v(u_1,u_2)e^{-2\pi i(k_1u_1+k_2u_2)}du_1du_2\\ &=\mathcal{F}[f(-x)](k_1+k_2)\mathcal{F}[v(u_1,u_2)](k_1,k_2)\\ &=\bar{\mathcal{F}}[f(x)](k_1+k_2)\mathcal{F}[v](k_1,k_2)\end{aligned} \tag{3.20}$$

where $\bar{z}$ denotes the complex conjugate of z.

By the properties of Fourier Transform (3.5), (3.6), (3.7) and (3.20), equation (3.17) can be simplified to:

$$\begin{aligned}\frac{\partial}{\partial\tau}\mathcal{F}[v](k_1,k_2)=&\frac{1}{2}\sigma_1^2(2\pi ik_1)^2\mathcal{F}[v](k_1,k_2)+\frac{1}{2}\sigma_2^2(2\pi ik_2)^2\mathcal{F}[v](k_1,k_2)\\ &+(r-\lambda\kappa-\frac{1}{2}\sigma_1^2)(2\pi ik_1)\mathcal{F}[v](k_1,k_2)+(r-\lambda\kappa-\frac{1}{2}\sigma_2^2)(2\pi ik_2)\mathcal{F}[v](k_1,k_2)\\ &+\rho\sigma_1\sigma_2(2\pi ik_1)(2\pi ik_2)\mathcal{F}[v](k_1,k_2)-(r+\lambda)\mathcal{F}[v](k_1,k_2)\\ &+\lambda\bar{\mathcal{F}}[f(x)](k_1+k_2)\mathcal{F}[v](k_1,k_2).\end{aligned} \tag{3.21}$$

Rearranging the terms in (3.21) gives:

$$
\begin{aligned}
\frac{\partial}{\partial \tau}\mathcal{F}[v](k_1,k_2) =&\mathcal{F}[v](k_1,k_2)\Big(-\frac{1}{2}\sigma_1^2(2\pi k_1)^2 - \frac{1}{2}\sigma_2^2(2\pi k_2)^2 \\
&+ (r-\lambda\kappa-\frac{1}{2}\sigma_1^2)(2\pi i k_1) + (r-\lambda\kappa-\frac{1}{2}\sigma_2^2)(2\pi i k_2) \\
&- \rho\sigma_1\sigma_2(2\pi k_1)(2\pi k_2) - (r+\lambda) + \lambda\bar{\mathcal{F}}[f(x)](k_1+k_2)\Big).
\end{aligned} \tag{3.22}
$$

Define $V(k_1,k_2) := \mathcal{F}[v](k_1,k_2)$, $F(k_1+k_2) := \mathcal{F}[f(x)](k_1+k_2)$ so that the derivative with respect to τ can be writtern as $V_\tau(k_1,k_2) := \frac{\partial}{\partial\tau}\mathcal{F}[v](k_1,k_2)$. In addition, define the *characteristic exponent* $\Psi(k_1,k_2)$ as:

$$
\begin{aligned}
\Psi(k_1,k_2) =& -\frac{1}{2}\sigma_1^2(2\pi k_1)^2 - \frac{1}{2}\sigma_2^2(2\pi k_2)^2 \\
&+ (r-\lambda\kappa-\frac{1}{2}\sigma_1^2)(2\pi i k_1) + (r-\lambda\kappa-\frac{1}{2}\sigma_2^2)(2\pi i k_2) \\
&- \rho\sigma_1\sigma_2(2\pi k_1)(2\pi k_2) - (r+\lambda) + \lambda\bar{\mathcal{F}}[f(x)](k_1+k_2).
\end{aligned} \tag{3.23}
$$

With these new notations, equation (3.22) can be rewritten as:

$$
0 = V_\tau(k_1,k_2) - V(k_1,k_2)\cdot\Psi(k_1,k_2). \tag{3.24}
$$

Hence, by using a change of variables and the properties of the Fourier transforms, the original PIDE (2.23) is converted into a linear ordinary differential equation (ODE) in τ given by (3.24). This ODE can be solved in closed-form in Fourier space and the option price in real space can be transformed back from Fourier space by taking the inverse Fourier transform.

3.4.2 Solving the Ordinary Differential Equation

By introducing the integrating factor $e^{-\Psi(k_1,k_2)\tau}$, the ODE (3.24) can be easily solved:

$$
\begin{aligned}
0 &= e^{-\Psi(k_1,k_2)\tau}V_\tau(k_1,k_2) - e^{-\Psi(k_1,k_2)\tau}V(k_1,k_2)\cdot\Psi(k_1,k_2) \\
&= \frac{\partial}{\partial\tau}\big(V(k_1,k_2)e^{-\Psi(k_1,k_2)\tau}\big).
\end{aligned} \tag{3.25}
$$

Integrating both sides of (3.25) with respect to τ:

$$
V(k_1,k_2) = C\cdot e^{\Psi(k_1,k_2)\tau}
$$

where C is constant.

Let $V^n(k_1, k_2) := \mathcal{F}[v(x_1, x_2, \tau)](k_1, k_2)$ denote the Fourier transform of the option price at time τ_n. Then for any $0 \le \tau_l \le \tau_u \le T$, given the Fourier transform of the option price at time τ_l, V^l, the Fourier transform of the option price at time τ_u can be computed by:

$$V^u(k_1, k_2) = V^l(k_1, k_2) \cdot e^{\Psi(k_1,k_2)(\tau_u - \tau_l)}. \tag{3.26}$$

The inverse Fourier transform can be applied on (3.26) to recover the option value:

$$v(x_1, x_2, \tau_u) = \mathcal{F}^{-1}\left[V^l(k_1, k_2) \cdot e^{\Psi(k_1,k_2)(\tau_u - \tau_l)}\right](x_1, x_2). \tag{3.27}$$

The equations (3.26) and (3.27) provide the main idea on how to time-step in Fourier space and recover the option prices in real space, using a continuous Fourier transform and its inverse.

3.4.3 Fourier Space Time-stepping

Note that equations (3.26) and (3.27) use the CFT and ICFT. In practice, DFT and IDFT are used to approximate CFT and ICFT to compute numerical solutions:

$$V^u(k_{1n_1}, k_{2n_2}) \approx e^{-i2\pi(k_{1n_1}+k_{2n_2})x_{min}} \cdot \Delta x_1 \Delta x_2 \cdot \hat{V}^u(n_1, n_2) \tag{3.28}$$

and

$$V^l(k_{1n_1}, k_{2n_2}) \approx e^{-i2\pi(k_{1n_1}+k_{2n_2})x_{min}} \cdot \Delta x_1 \Delta x_2 \cdot \hat{V}^l(n_1, n_2). \tag{3.29}$$

Therefore, equation (3.26) can be approximated by using (3.28) and (3.29), which after eliminating factors of $e^{-i2\pi(k_{1n_1}+k_{2n_2})x_{min}} \cdot \Delta x_1 \Delta x_2$ gives:

$$\hat{V}^u(n_1, n_2) = \hat{V}^l(n_1, n_2) \cdot e^{\Psi(k_1,k_2)(\tau_u - \tau_l)}. \tag{3.30}$$

The inverse discrete Fourier transform (IDFT) can be used to transform the option price in real space back, for any $m_1, m_2 = 0, 1, \cdots, N-1$:

$$\begin{aligned} IDFT\left[\hat{V}^u(n_1, n_2)\right](x_{1m_1}, x_{2m_2}) &= IDFT\left[\hat{V}^l(n_1, n_2) \cdot e^{\Psi(k_1,k_2)(\tau_u - \tau_l)}\right](x_{1m_1}, x_{2m_2}) \\ v(x_{1m_1}, x_{2m_2}, \tau_u) &= IDFT\left[e^{\Psi(k_1,k_2)(\tau_u - \tau_l)} \cdot DFT\left[v(x_{1m_1}, x_{2m_2}, \tau_l)\right]\right]. \end{aligned} \tag{3.31}$$

Here, the computed value $v(x_{1m_1}, x_{2m_2}, \tau_u)$ represents the option price when the underlying prices are $(S_1, S_2) = (e^{x_{1m_1}}, e^{x_{2m_2}})$ at time τ_u.

3.4.4 Illustration of Method

To price the options under the shared-jump model, the FST method can be implemented to solve the PIDE given by equation (2.23) numerically.

The underlying prices domain (S_1, S_2) is discretized by defining nodes in both of the (S_1, S_2) directions denoted as $[S_{1_0}, S_{1_1}, \cdots, S_{1_{max}}] \times [S_{2_0}, S_{2_1}, \cdots, S_{2_{max}}]$, which are equally spaced in log space $(\log(S_1), \log(S_2))$.

For European options, there are no conditions imposed on the option until the expiry date. Hence, the time domain can be discretized as $\tau^0 = 0, \tau^1 = T$ so that $\Delta\tau = T$. By using the FST method, European options can be priced with only one time-step, from $\tau^0 = 0$ to $\tau^1 = T$.

For American options, the time domain should be discretized as $[\tau^0 = 0, \tau^1, \cdots, \tau^M = T]$ with $\Delta\tau = \frac{T}{M}$ in order to take the early exercise boundary into consideration. When using the FST method, the computed option price needs to be updated during each time-step by checking the possibility of early exercise.

Chapter 4

Numerical Results

4.1 One-factor Jump Diffusion Cases

Under the one-factor jump diffusion model, the options pricing PIDE is given by equation (2.2):

$$\mathcal{V}_\tau = \frac{\sigma^2 S^2}{2}\mathcal{V}_{SS} + (r - \lambda\kappa)S\mathcal{V}_S - (r+\lambda)\mathcal{V} + \Big(\lambda\int_0^\infty \mathcal{V}(S\eta)g(\eta)d\eta\Big).$$

After doing a log transformation and Fourier transform, the *characteristic exponent* can be obtained as:

$$\Psi(k) = -\frac{\sigma^2}{2}(2\pi k)^2 + (r - \lambda\kappa - \frac{\sigma^2}{2})(2\pi ik) - (r+\lambda) + \lambda\bar{F}(k) \tag{4.1}$$

where $F(k)$ is defined as the Fourier transform of the jump density function $f(x)$ and the derivation of $F(k)$ can be found in (Appendix A). In addition, $\bar{z}$ denotes the complex conjugate of z.

Precisely speaking, for the Merton jump density, we have

$$f(y) = \frac{1}{\sqrt{2\pi}\gamma}e^{-\frac{1}{2}(\frac{y-\mu}{\gamma})^2},\ F(k) = e^{-2(\pi ik\mu+(\pi k\gamma)^2)}. \tag{4.2}$$

For the Kou jump density, we get

$$f(y) = p\eta_1 e^{-y\eta_1}\cdot 1_{\{y\geq 0\}} + (1-p)\eta_2 e^{y\eta_2}\cdot 1_{\{y\leq 0\}},\ F(k) = \frac{p}{1+2\pi ik(\frac{1}{\eta_1})} + \frac{1-p}{1-2\pi ik(\frac{1}{\eta_2})}. \tag{4.3}$$

4.1.1 Pricing Results

Table (4.1) shows the parameters for a European put under a one-factor jump diffusion model with the Merton jump density. The pricing results are listed in Table (4.2).

Parameters	Value
S	100
K	110
r	0.05
q^1	0.02
T	10
σ	0.15
λ	0.1
μ	-1.08
γ	0.4

Table 4.1: Parameters for a European put under the one-factor Merton jump diffusion model

Refinement	Nodes	Price[2]	Change	Ratio[3]
0	512	18.00485074		
1	1024	18.00393356	0.00091718	
2	2048	18.00370453	0.00022903	4.00462736
3	4096	18.00364730	0.00005722	4.00229568
4	8192	18.00363300	0.00001430	4.00114271
5	16384	18.00362943	0.00000358	4.00056890

Table 4.2: Pricing results of a European put under the one-factor Merton jump diffusion model: $[x_{min}, x_{max}] = [-7.5, 7.5]$

As shown in Tables (4.1) and (4.2), second order convergence is obtained for pricing a European put under the one-factor Merton jump diffusion model by FST method.

[1]Note that q is the continuous dividend rate, which shrinks risk-free rate r.

[2]Reference price of 18.00362936 is given by Surkov (2009)[17].

[3]Denote the option prices as $V_1, V_2, \cdots, V_6$, then the changes are defined as $V_1 - V_2, V_2 - V_3, \cdots, V_5 - V_6$, and ratios are defined as $\frac{V_1-V_2}{V_2-V_3}, \frac{V_2-V_3}{V_3-V_4}, \cdots, \frac{V_5-V_6}{V_4-V_5}$. Therefore, the binary logarithm of a ratio shows the numerical order of convergence.

Table (4.3) shows the parameters for a European call under a one-factor jump diffusion model with the Kou jump density. The pricing results are shown in Table (4.4).

Parameters	Value
S	100
K	110
r	0
T	1
σ	0.2
λ	0.2
p	0.5
η_1	3
η_2	2

Table 4.3: Parameters for a European call under the one-factor Kou jump diffusion model

Refinement	Nodes	Price[4]	Change	Ratio
0	512	7.30281862		
1	1024	7.28243068	0.02038794	
2	2048	7.28161780	0.00081288	25.08114610
3	4096	7.28035126	0.00126654	0.64181120
4	8192	7.28003467	0.00031660	4.00048234
5	16384	7.27995551	0.00007916	3.99940610

Table 4.4: Pricing results of a European call under the one-factor Kou jump diffusion model: $[x_{min}, x_{max}] = [-7.5, 7.5]$

As shown in Tables (4.3) and (4.4), second order convergence is obtained as well for pricing a European call under the one-factor Kou jump diffusion model by FST method.

4.1.2 Wrap-around Error

When implementing the FST method, a periodic domain is assumed implicitly, while the domain of the log underlying prices is actually aperiodic. Hence, the periodic assumption

[4] Reference price of 7.27993383 is given by Surkov (2009).

causes option values on the ends of the grid to be wrapped around to the other side of the grid. This produces spurious solutions near both left and right ends.

The simple cure to remedy the wrap-around error is zero padding. For the domain of the log underlying prices, zeros are added and the Fourier transform is done on a grid with the size twice as the original length. At the same time, in the Fourier domain, the number of nodes is doubled as well. Then during the FST process, after applying the inverse Fourier transform, the added zeros are removed.

In detail, let $\mathcal{V}(S_i, \tau^m)$ denote the option value at node $S_i, i = 0, 1, \cdots, N-1$, at time τ^m. So, without padding, the Fourier transform is applied to the vector $\mathcal{V}^m$:

$$\mathcal{V}^m = [\underbrace{\mathcal{V}(S_0, \tau^m), \mathcal{V}(S_1, \tau^m), \cdots, \mathcal{V}(S_{N-1}, \tau^m)}_{N}]$$

where N is the total number of nodes in the S direction. When using zero padding, the new vector $\hat{\mathcal{V}}^m$ is constructed by adding zero nodes to both ends of $\mathcal{V}^m$ in the S direction:

$$\hat{\mathcal{V}}^m = [\underbrace{0, \cdots, 0}_{\frac{N}{2}}, \underbrace{\mathcal{V}(S_0, \tau^m), \mathcal{V}(S_1, \tau^m), \cdots, \mathcal{V}(S_{N-1}, \tau^m)}_{N}, \underbrace{0, \cdots, 0}_{\frac{N}{2}}].$$

However, zero padding is not accurate enough since there may still have a huge gap between zeros and the values on the end, which leads to spurious results. Therefore, constant padding is introduced in this part.

For constant padding, rather than adding zeros to the original vector $\mathcal{V}^m$, the values on the very left and right ends are used to expand the domain. Define constants $c_l^m = \mathcal{V}(S_0, \tau^m)$ and $c_r^m = \mathcal{V}(S_{N-1}, \tau^m)$, then the brand new vector $\tilde{\mathcal{V}}^m$ is constructed as follows:

$$\tilde{\mathcal{V}}^m = [\underbrace{c_l^m, \cdots, c_l^m}_{\frac{N}{2}}, \underbrace{c_l^m = \mathcal{V}(S_0, \tau^m), \mathcal{V}(S_1, \tau^m), \cdots, \mathcal{V}(S_{N-1}, \tau^m) = c_r^m}_{N}, \underbrace{c_r^m, \cdots, c_r^m}_{\frac{N}{2}}].$$

Take the European options as an example. In the log underlying price domain, the differences between the zero padding and constant padding are presented in Figure (4.1) and Figure (4.2).

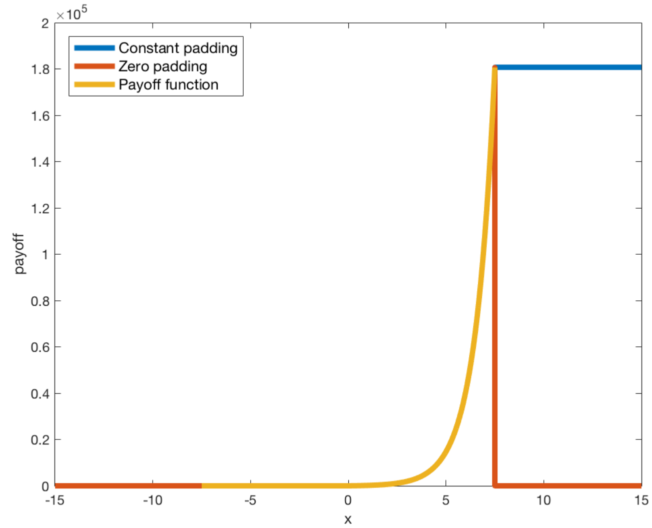

Figure 4.1: European call option pricing using zero padding and constant padding

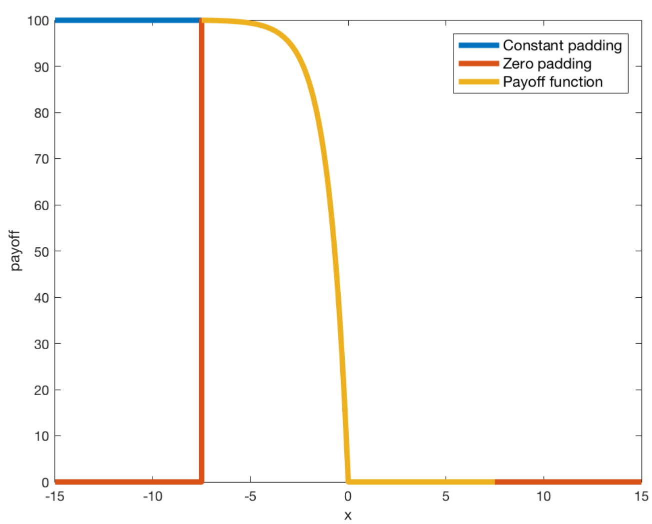

Figure 4.2: European put option pricing using zero padding and constant padding

In practice, it is of interest to focus on the option value when the underlying price tends to be zero rather than extremely large. Since the payoff function of European call option is always zero near the left end, it is almost the same for zero padding and constant padding. However, constant padding is significantly different from zero padding for the European put option.

The parameters for a European put under the one-factor jump diffusion model with the Merton jump density are displayed in Table (4.5).

Parameters	Value
S	100
K	100
r	0.1
q	0.02
T	1
σ	0.2
λ	0.1
μ	-0.5
γ	0.45

Table 4.5: Parameters for wrap-around analysis: a European put option

In this case, the domain of the log underlying prices is defined as Se^x rather than e^x in order to make the grid centered at $S = K = 100$. So, when using the zero padding and constant padding, the original domain $\Omega = [x_{min}, x_{max}] = [-7.5, 7.5]$ is expanded into $\tilde{\Omega} = [x'_{min}, x'_{max}] = [-15, 15]$. In addition, the total number of nodes in Ω is $N = 16384$. Therefore, $\tilde{\Omega}$ contains $2N = 32768$ nodes in total.

S	No padding	Zero padding	Constant padding	Closed-form solution
0.1	87.18014225	87.17857200	90.38700804	90.38572194
1	89.50246250	89.50246152	89.50354351	89.50354313
10	80.68175406	80.68175401	80.68175411	80.68175514
100	5.94853212	5.94853211	5.94853211	5.94851381
1000	0.00211219	0.00211219	0.00211219	0.00211218
10000	0.00000024	0.00000023	0.00000023	0.00000023
100000	0.68766360	0.00000000	0.00000000	0.00000000

Table 4.6: Effect of wrap-around error on the value of a European put option: *zero padding* and *constant padding*

As shown in Table (4.6), the option price tends to be incorrect on both ends without padding. Even though zero padding can reduce the effect of wrap-around on the right end, it cannot fix the problem on the left end. Last but not least, constant padding performs best among all three methods for eliminating the wrap-around error for both ends.

Besides zero padding and constant padding, asymptotic padding is another promising choice to extend the domain of log underlying prices and reduce the wrap-around error. Take a European call option as an example. Since the log transformation gives $x = \log(\frac{S}{K})$ and $S = Ke^x$, the payoff function of a European call option can be written as:

$$\begin{aligned}\mathcal{V}(x,0) &= \mathcal{V}(S,0)\\ &= \max(S-K,0)\\ &= \max(Ke^x-K,0)\\ &= \max(K(e^x-1),0).\end{aligned}$$

By the Taylor expansions for the exponential function at $x = x_0$:

$$\begin{aligned}e^x &= e^{x_0} + \frac{e^{x_0}}{1!}(x-x_0) + \frac{e^{x_0}}{2!}(x-x_0)^2 + \frac{e^{x_0}}{3!}(x-x_0)^3 + \cdots\\ &= e^{x_0}\Big(1 + \frac{(x-x_0)}{1!} + \frac{(x-x_0)^2}{2!} + \frac{(x-x_0)^3}{3!} + \cdots\Big),\end{aligned} \tag{4.4}$$

the asymptotic extension of log underlying prices domain for the right end can be easily derived by taking $x_0 = x_{max}$: $K\Big(e^{x_{max}}\big(1 + \frac{(x-x_{max})}{1!} + \frac{(x-x_{max})^2}{2!} + \frac{(x-x_{max})^3}{3!} + \cdots\big) - 1\Big)$, where K is the strike price and x_{max} is the right end point of the log prices domain. As for the left end, it is straightforward to simply use zero padding since the value of a European call option is always zero when $S \leq K$.

Furthermore, zero padding can be seen as using zero term from asymptotic padding while constant padding can be viewed as using only first term from asymptotic padding. If the first two terms are used, then linear trend of log underlying prices on the right side will be captured by asymptotic padding. Similarly, if the first three terms are used, then both of linear and quadratic properties can be reflected. Figure (4.3) displays the differences between asymptotic padding using one (constant), two (linear) and three (quadratic) terms.

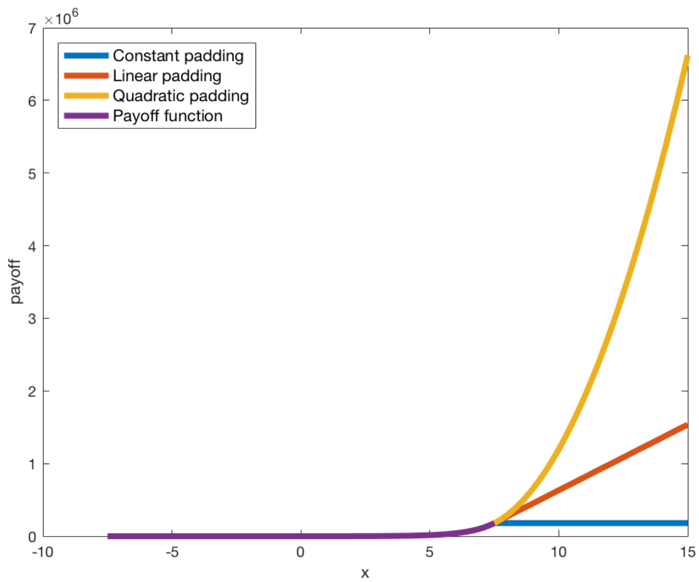

Figure 4.3: European call option pricing using asymptotic padding

The parameters for a European call under the one-factor jump diffusion model with the Merton jump density are shown in Table (4.7).

Parameters	Value
S	100
K	100
r	0.05
q	0.01
T	1
σ	0.4
λ	0.2
μ	-0.45
γ	0.5

Table 4.7: Parameters for wrap-around analysis: a European call option

In this example, the original domain $\Omega = [x_{min}, x_{max}] = [-7.5, 7.5]$ is expanded into $\tilde{\Omega} = [x'_{min}, x'_{max}] = [-15, 15]$. The total number of nodes in Ω is $N = 8192$. Therefore, $\tilde{\Omega}$ contains $2N = 16384$ nodes in total. The results for asymptotic padding can be found in Table (4.8).

S	Constant padding	Linear padding	Quadratic padding	Closed-form solution
0.1	0.00000043	0.00000352	0.00001474	0.00000000
1	0.00000000	0.00000000	0.00000000	0.00000000
10	0.00003847	0.00003847	0.00003847	0.00003847
100	18.86737568	18.86737568	18.86737568	18.86730167
1000	885.10319389	885.10319389	885.10319389	885.10310367
10000	9706.86630576	9706.86748324	9706.86765999	9706.86380538
100000	95250.91437482	97462.61113516	97848.56616981	97924.74438823

Table 4.8: Effect of wrap-around error on the value of a European call option: *asymptotic padding*

It can be seen from Table (4.8) that there exists a tradeoff between the wrap-around error on the left and right ends. The more terms used in asymptotic padding, the computed option values are more accurate on the right end while less accurate on the left end.

Last but not least, the extension of log underlying prices domain is not necessary to be symmetric. Since the Fourier transform assumes a periodic domain implicitly, the extension of domain in current period may be shifted to next period. For example, when using zero padding, the vector $\mathcal{V}^m$ is extended into a new vector $\hat{\mathcal{V}}^m$:

$$\hat{\mathcal{V}}^m = [\underbrace{0, \cdots, 0}_{\frac{N}{2}}, \underbrace{\mathcal{V}(S_0, \tau^m), \mathcal{V}(S_1, \tau^m), \cdots, \mathcal{V}(S_{N-1}, \tau^m)}_{N}, \underbrace{0, \cdots, 0}_{\frac{N}{2}}].$$

It is equivalent to shifting all the zeros on the left end to the right end:

$$\hat{\mathcal{V}}^m = [\underbrace{\mathcal{V}(S_0, \tau^m), \mathcal{V}(S_1, \tau^m), \cdots, \mathcal{V}(S_{N-1}, \tau^m)}_{N}, \underbrace{0, \cdots, 0}_{N}].$$

4.2 Two-factor Jump Diffusion Cases

As before, under the two-factor jump diffusion model, the options pricing PIDE is given by equation (2.8):

$$\begin{aligned}\mathcal{V}_\tau =& \frac{\sigma_1^2 S_1^2}{2}\mathcal{V}_{S_1S_1} + \frac{\sigma_2^2 S_2^2}{2}\mathcal{V}_{S_2S_2} + (r-\lambda_1\kappa_1)S_1\mathcal{V}_{S_1} + (r-\lambda_2\kappa_2)S_2\mathcal{V}_{S_2} + \rho\sigma_1\sigma_2 S_1S_2\mathcal{V}_{S_1S_2} \\ & - (r+\lambda_1+\lambda_2)\mathcal{V} + \Big(\lambda_1\int_0^\infty \mathcal{V}(S_1\eta_1)g(\eta_1)d\eta_1\Big) + \Big(\lambda_2\int_0^\infty \mathcal{V}(S_2\eta_2)g(\eta_2)d\eta_2\Big).\end{aligned}$$

After log transformation and Fourier transform, the *characteristic exponent* can be derived as follows:

$$\begin{aligned}\Psi(k_1,k_2) =& -\frac{\sigma_1^2}{2}(2\pi k_1)^2 - \frac{\sigma_2^2}{2}(2\pi k_2)^2 + (r-\lambda_1\kappa_1-\frac{\sigma_1^2}{2})(2\pi i k_1) + (r-\lambda_2\kappa_2-\frac{\sigma_2^2}{2})(2\pi i k_2) \\ & + \rho\sigma_1\sigma_2(2\pi k_1)(2\pi k_2) - (r+\lambda_1+\lambda_2) + \lambda_1\bar{F}_1(k_1) + \lambda_2\bar{F}_2(k_2).\end{aligned} \tag{4.5}$$

The independent jump density is given by equations (4.2) and (4.3).

4.2.1 Pricing Results

Table (4.9) gives the parameters for a European spread call under the two-factor jump diffusion model with the Merton jump density. The pricing results are presented in Table (4.10).

Parameters	Value
S_1, S_2	100
σ_1	0.1
σ_2	0.2
λ_1	0.25
λ_2	0.5
μ_1	0.13
μ_2	0.11
γ_1	0.37
γ_2	0.41
q_1, q_2	0.05
B_1, B_2	1
T	1
K	2
r	0.1
ρ	0.5

Table 4.9: Parameters for a European spread call under the two-factor Merton jump diffusion model

Refinement	Nodes	Price[5]	Change	Ratio
0	512^2	13.74164280		
1	1024^2	13.72000852	0.02163429	
2	2048^2	13.71519276	0.00481576	4.49239252
3	4096^2	13.71392828	0.00126448	3.80850192
4	8192^2	13.71363235	0.00029593	4.27284272

Table 4.10: Pricing results of a European spread call under the two-factor Merton jump diffusion model: $[x_{min}, x_{max}]^2 = [-7.5, 7.5]^2$

As shown in Tables (4.9) and (4.10), the order of convergence is approximately 2 in space for pricing a European spread call under the two-factor Merton jump diffusion model by the FST method.

[5]Reference price of 13.714948858 is given by Surkov (2009).

4.2.2 Wrap-around Error

From one-dimensional to two-dimensional cases, wrap-around error will also occur when implementing the FST method. Continually with the idea of constant padding in one-factor case, two-dimensional constant padding can be introduced as follows.

Let $\mathcal{V}_{i,j}^m := \mathcal{V}(S_{1_i}, S_{2_j}, \tau^m)$ denote the option value at node (S_{1_i}, S_{2_j}), where $i, j = 0, 1, \cdots, N-1$ at time τ^m. Without padding, the two-dimensional Fourier transform is applied to the $N \times N$ matrix $\mathcal{V}^m$:

$$\mathcal{V}^m = \begin{bmatrix} \mathcal{V}_{0,0}^m & \cdots & \mathcal{V}_{N-1,0}^m \\ \vdots & \ddots & \vdots \\ \mathcal{V}_{0,N-1}^m & \cdots & \mathcal{V}_{N-1,N-1}^m \end{bmatrix}.$$

In order to use constant padding in the two-dimensional case, the original matrix $\mathcal{V}^m$ can be expanded into a new $2N \times 2N$ matrix $\tilde{\mathcal{V}}^m$:

$$\tilde{\mathcal{V}}^m = \begin{bmatrix} \mathcal{M}_1^m & \mathcal{M}_2^m & \mathcal{M}_3^m \\ \mathcal{M}_4^m & \mathcal{V}^m & \mathcal{M}_5^m \\ \mathcal{M}_6^m & \mathcal{M}_7^m & \mathcal{M}_8^m \end{bmatrix}$$

where $\mathcal{M}_1^m, \mathcal{M}_3^m, \mathcal{M}_6^m$ and $\mathcal{M}_8^m$ are all $\frac{N}{2} \times \frac{N}{2}$ constant matrices:

$$\mathcal{M}_1^m = \begin{bmatrix} \mathcal{V}_{0,0}^m \cdots \mathcal{V}_{0,0}^m \\ \vdots \ddots \vdots \\ \mathcal{V}_{0,0}^m \cdots \mathcal{V}_{0,0}^m \end{bmatrix}, \mathcal{M}_3^m = \begin{bmatrix} \mathcal{V}_{N-1,0}^m \cdots \mathcal{V}_{N-1,0}^m \\ \vdots \ddots \vdots \\ \mathcal{V}_{N-1,0}^m \cdots \mathcal{V}_{N-1,0}^m \end{bmatrix},$$

$$\mathcal{M}_6^m = \begin{bmatrix} \mathcal{V}_{0,N-1}^m \cdots \mathcal{V}_{0,N-1}^m \\ \vdots \ddots \vdots \\ \mathcal{V}_{0,N-1}^m \cdots \mathcal{V}_{0,N-1}^m \end{bmatrix}, \mathcal{M}_8^m = \begin{bmatrix} \mathcal{V}_{N-1,N-1}^m \cdots \mathcal{V}_{N-1,N-1}^m \\ \vdots \ddots \vdots \\ \mathcal{V}_{N-1,N-1}^m \cdots \mathcal{V}_{N-1,N-1}^m \end{bmatrix}.$$

$\mathcal{M}_2^m$ and $\mathcal{M}_7^m$ are $\frac{N}{2} \times N$ matrices with same values for each row:

$$\mathcal{M}_2^m = \begin{bmatrix} \mathcal{V}_{0,0}^m & \cdots & \mathcal{V}_{N-1,0}^m \\ \vdots & \ddots & \vdots \\ \mathcal{V}_{0,0}^m & \cdots & \mathcal{V}_{N-1,0}^m \end{bmatrix}, \mathcal{M}_7^m = \begin{bmatrix} \mathcal{V}_{0,N-1}^m & \cdots & \mathcal{V}_{N-1,N-1}^m \\ \vdots & \ddots & \vdots \\ \mathcal{V}_{0,N-1}^m & \cdots & \mathcal{V}_{N-1,N-1}^m \end{bmatrix}.$$

$\mathcal{M}_4^m$ and $\mathcal{M}_5^m$ are $N \times \frac{N}{2}$ matrices with same values for each column:

$$\mathcal{M}_4^m = \begin{bmatrix} \mathcal{V}_{0,0}^m & \cdots & \mathcal{V}_{0,0}^m \\ \vdots & \ddots & \vdots \\ \mathcal{V}_{0,N-1}^m & \cdots & \mathcal{V}_{0,N-1}^m \end{bmatrix}, \mathcal{M}_5^m = \begin{bmatrix} \mathcal{V}_{N-1,0}^m & \cdots & \mathcal{V}_{N-1,0}^m \\ \vdots & \ddots & \vdots \\ \mathcal{V}_{N-1,N-1}^m & \cdots & \mathcal{V}_{N-1,N-1}^m \end{bmatrix}.$$

Intuitively, the idea for constant padding can be described by Figure (4.4):

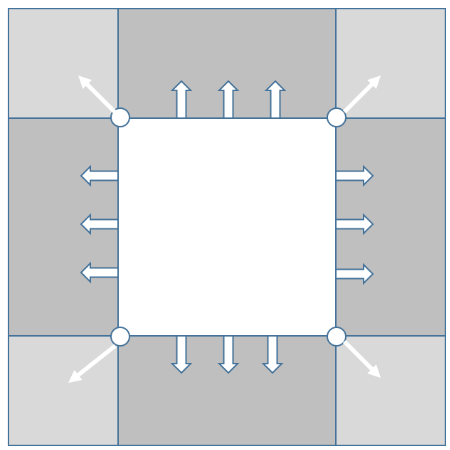

Figure 4.4: Intuitive idea for constant padding in two dimensions

Using the European spread call example shown above, the parameters are listed in Table (4.9). The original domain $\Omega = [x_{min}, x_{max}]^2 = [-7.5, 7.5]^2$ is expanded into $\tilde{\Omega} = [x'_{min}, x'_{max}]^2 = [-15, 15]^2$. In addition, the total number of nodes in Ω is $N^2 = 1024^2$. Therefore, $\tilde{\Omega}$ contains $(2N)^2 = 2048^2$ nodes in total.

The effect of the wrap-around error and the reduction in wrap-around error by using constant padding on the European spread call are displayed in Table (4.11) and Table (4.12).

	S_2	0.1	1	10	100	1000	10000	100000
S_1	x	-6.9078	-4.6052	-2.3026	0	2.3026	4.6052	6.9078
0.1	-6.9078	5003.73181862	0.05921847	7.44390359	91.20579832	928.82572488	9303.91456738	80823.40168517
1	-4.6052	5128.71781581	0.04504810	6.75280164	92.36455481	948.49374193	9508.64663690	82598.33708319
10	-2.3026	5128.40582923	0.03699906	0.93341120	83.80336239	939.93259791	9500.08689466	82590.27233297
100	0	5125.27577522	0.03686791	0.00220805	13.72001200	854.32012750	9414.47442373	82509.49357610
1000	2.3026	5093.97524082	0.03665502	0.00000079	0.02411654	143.05136774	8558.35440025	81701.70615469
10000	4.6052	4780.97012512	0.03452676	0.00000005	0.00000771	0.24331756	1435.34375033	73623.88083482
100000	6.9078	1763.14404756	0.01408759	0.07856428	0.94778356	9.64004627	98.37997582	8032.19200756

Table 4.11: Effect of wrap-around error on the value of a European spread call option: *no padding*

	S_2	0.1	1	10	100	1000	10000	100000
S_1	x	-6.9078	-4.6052	-2.3026	0	2.3026	4.6052	6.9078
0.1	-6.9078	0.00000151	0.02374630	7.60764247	93.22048366	949.34861339	9510.32960373	91519.18921942
1	-4.6052	0.00000040	0.00815625	6.75279563	92.36457173	948.49270146	9509.47369181	91518.33330749
10	-2.3026	0.00000000	0.00010992	0.93339475	83.80337167	939.93141440	9500.91240475	91509.77202044
100	0	0.00000000	0.00000007	0.00220796	13.72000852	854.31893468	9415.29944524	91424.15906093
1000	2.3026	0.00000000	0.00000000	0.00000075	0.02411624	143.04821613	8559.17583924	90568.03092627
10000	4.6052	0.00000000	0.00000000	0.00000000	0.00000759	0.24331583	1436.03933065	82006.83260731
100000	6.9078	0.00000000	0.00000000	0.00000000	0.00000000	0.00007108	2.17400700	10778.18364481

Table 4.12: Effect of wrap-around error on the value of a European spread call option: *constant padding*

As shown in Table (4.11) and Table (4.12), the option values on the edges of the matrix seem to be incorrect without padding. After using constant padding, however, these values tend to be reasonable.

4.3 Shared-jump Diffusion Cases

As mentioned before in Section 3.4, the *characteristic exponent* under the shared-jump diffusion model is given by equation (3.23):

$$\begin{aligned}\Psi(k_1,k_2) = &-\frac{1}{2}\sigma_1^2(2\pi k_1)^2 - \frac{1}{2}\sigma_2^2(2\pi k_2)^2 \\ &+ (r-\lambda\kappa-\frac{1}{2}\sigma_1^2)(2\pi i k_1) + (r-\lambda\kappa-\frac{1}{2}\sigma_2^2)(2\pi i k_2) \\ &- \rho\sigma_1\sigma_2(2\pi k_1)(2\pi k_2) - (r+\lambda) + \lambda\bar{\mathcal{F}}[f(x)](k_1+k_2).\end{aligned}$$

In addition, the jump density is given by equation (4.3).

4.3.1 Pricing Results

The parameters for a European spread call under the shared-jump diffusion model with Kou jump density are shown in Table (4.13) and the pricing results are presented in Table (4.14).

Parameters	Value
S_1, S_2	100
σ_1	0.1
σ_2	0.2
λ	1
p	0.4
η_1	3
η_2	2
B_1, B_2	1
T	1
K	2
r	0.1
ρ	0.5

Table 4.13: Parameters for a European spread call under the shared-jump diffusion model

Refinement	Nodes	Price	Change	Ratio
0	512^2	6.16739294		
1	1024^2	6.12648119	0.04091174	
2	2048^2	6.11736900	0.00911220	4.489778638
3	4096^2	6.11499200	0.00237700	3.833485132
4	8192^2	6.11441482	0.00057717	4.118356562

Table 4.14: Pricing results of a European spread call under the shared-jump diffusion model: *FST method*, $[x_{min}, x_{max}]^2 = [-7.5, 7.5]^2$

Tables (4.13) and (4.14) demonstrate that second order convergence is attained for pricing a European spread call under the shared-jump diffusion model by the FST method.

4.3.2 Monte Carlo Results

In order to check the results by FST method, Monte Carlo simulation is used to price the same European spread call under the shared-jump diffusion model.

The Monte Carlo approach for option pricing was firstly introduced by Boyle (1977)[4]. Monte Carlo method simulates the process generating the returns on the underlying asset and invokes the risk neutrality assumption to derive the value of the option.

Note that using forward Euler to approximate the SDEs has $\mathcal{O}(\Delta t)$ truncation error while Monte Carlo simulation has $\mathcal{O}(\frac{1}{\sqrt{M}})$ error, where Δt is the timestep and M is the total number of Monte Carlo paths. Thus, there are two sources of error in Monte Carlo approach: time-stepping error and sampling error:

$$error = \mathcal{O}\Big(\max(\Delta t, \frac{1}{\sqrt{M}})\Big) \tag{4.6}$$

Equation (4.6) shows that it is crucial to balance time-stepping error and sampling error when using Monte Carlo. In order to make these two errors the same order, M should be chosen as $\mathcal{O}(\frac{1}{(\Delta t)^2})$.

The details about the methodology of Monte Carlo simulation under the shared-jump diffusion model can be found in (Appendix C). The results derived by Monte Carlo simulations are provided in Table (4.15).

Simulations	Timesteps	Price	Stdev	95% CI[6]
100000	1600	6.10757277	0.04689684	[6.0157,6.1995]
400000	3200	6.11528466	0.02473321	[6.0668,6.1638]
1600000	6400	6.12621791	0.01166751	[6.1033,6.1491]
6400000	128000	6.11290968	0.00583618	[6.1015,6.1243]
25600000	256000	6.11145233	0.00298162	[6.1056,6.1173]

Table 4.15: Pricing results of a European spread call under the shared-jump diffusion model: *Monte Carlo simulation*

By comparing the results in Table (4.14) and Table (4.15), the FST method (6.11441482) is consistent with Monte Carlo simulations.

4.3.3 Wrap-around Error

When using constant padding to reduce the wrap-around error under the shared-jump diffusion model, another issue is about jump density grid. The equation (3.23) gives the *characteristic exponent* :

$$\begin{aligned}\Psi(k_1,k_2) =& -\frac{1}{2}\sigma_1^2(2\pi k_1)^2 - \frac{1}{2}\sigma_2^2(2\pi k_2)^2 \\ &+ (r-\lambda\kappa-\frac{1}{2}\sigma_1^2)(2\pi i k_1) + (r-\lambda\kappa-\frac{1}{2}\sigma_2^2)(2\pi i k_2) \\ &- \rho\sigma_1\sigma_2(2\pi k_1)(2\pi k_2) - (r+\lambda) + \lambda\bar{\mathcal{F}}[f(x)](k_1+k_2).\end{aligned}$$

In the frequency domain, $k_1, k_2 \in \left\{\frac{-\frac{N}{2}+1}{x_{max}-x_{min}}, \cdots, \frac{\frac{N}{2}}{x_{max}-x_{min}}\right\}$ by equations (3.10) and (3.11). Since the Fourier transform of jump density is evaluated at (k_1+k_2), the range of its grid is doubled naturally when evaluating $\bar{\mathcal{F}}[f(x)](k_1+k_2)$ under the shared-jump diffusion model.

Especially, when using the constant padding, suppose the log underlying domain $\Omega = [x_{min}, x_{max}]^2$ is expanded into $\tilde{\Omega} = [x'_{min}, x'_{max}]^2 = [2x_{min}, 2x_{max}]^2$, the grid for the Fourier transform of jump density has to be quadrupled in order to evaluate $\bar{\mathcal{F}}[f(x)](k_1+k_2)$. Once $\Psi(k_1,k_2)$ is computed, however, only a doubled domain is required.

[6] The 95% confidence interval (CI) is constructed as $[\bar{x} - 1.96\frac{\sigma}{\sqrt{n}}, \bar{x} + 1.96\frac{\sigma}{\sqrt{n}}]$, where $\bar{x}$ denotes the sample mean, σ denotes the sample standard deviation and n represents the sample size.

Take the European spread put as an example, with the parameters listed in Table (4.16). In addition, the original domain $\Omega = [x_{min}, x_{max}]^2 = [-15, 15]^2$ is expanded into $\tilde{\Omega} = [x'_{min}, x'_{max}]^2 = [2x_{min}, 2x_{max}]^2 = [-30, 30]^2$. Also, the total number of nodes in Ω is $N^2 = 4096^2$. Therefore, $\tilde{\Omega}$ contains $(2N)^2 = 8192^2$ nodes in total.

Parameters	Value
S_1, S_2	100
σ_1	0.15
σ_2	0.2
λ	0.1
p	0.3
η_1	2.0
η_2	1.5
B_1, B_2	1
T	1
K	2
r	0.15
ρ	0.45

Table 4.16: Parameters for wrap-around analysis: a European spread put option

The effect of the wrap-around error and the reduction in wrap-around error by using constant padding on a European spread put under the shared-jump model are displayed in Table (4.17) and Table (4.18).

	S_2	0.1	1	10	100	1000	10000	100000
S_1	x	-6.9078	-4.6052	-2.3026	0	2.3026	4.6052	6.9078
0.1	-6.9078	17.47053985	75.23962310	74.69524146	74.69237973	74.69224819	74.69224357	74.69223950
1	-4.6052	4.97531710	2.27490574	2.61650451	2.62206396	2.62196232	2.62196013	2.62198299
10	-2.3026	11.71229797	10.80384886	1.95910322	0.09157702	0.09177131	0.09179222	0.09202230
100	0	101.62461135	100.72457649	91.72423190	8.43379086	0.00322242	0.00347426	0.00577647
1000	2.3026	1001.62690318	1000.72689799	991.72684943	901.72692206	75.97650618	0.00256109	0.02558471
10000	4.6052	10001.65778128	10000.75777909	9991.75775362	9901.75805724	9001.75485603	751.64060973	0.22998980
100000	6.9078	99999.24378477	99998.34381015	99989.34399198	99899.34636822	98999.36389335	89999.53747492	7506.43311041

Table 4.17: Effect of wrap-around error on the value of a European spread put option: *no padding*

	S_2	0.1	1	10	100	1000	10000	100000
S_1	x	-6.9078	-4.6052	-2.3026	0	2.3026	4.6052	6.9078
0.1	-6.9078	1.72141966	0.83609664	0.00400877	0.00014001	0.00000494	0.00000018	0.00000000
1	-4.6052	2.62142170	1.72176427	0.00465273	0.00014199	0.00000494	0.00000018	0.00000000
10	-2.3026	11.62147615	10.72147038	1.93974960	0.00016483	0.00000501	0.00000017	-0.00000001
100	0	101.62141429	100.72140853	91.72135410	8.43311492	0.00000580	0.00000018	0.00000001
1000	2.3026	1001.62730149	1000.72729573	991.72724130	901.72730316	75.97802593	0.00000022	0.00000003
10000	4.6052	10001.66539113	10000.76538538	9991.76533095	9901.76539282	9001.75950816	751.61329813	-0.00000001
100000	6.9078	100000.35849738	99999.45849163	99990.45843721	99900.45849907	99000.45261442	90000.41476119	7505.58978783

Table 4.18: Effect of wrap-around error on the value of a European spread put option: *constant padding*

Table (4.17) and Table (4.18) demonstrate that the option values on the edges of the matrix become reasonable after using the constant padding.

It is known that two key factors have influence on the accuracy of constant padding. One is the total number of nodes while the other is the length of the domain. In order to have a better understanding of the accuracy of constant padding, the convergence of the option value at $(S_1, S_2) = (100, 100)$ under two different cases are shown in Table (4.19) and Table (4.20).

On one hand, the domain $\Omega = [x_{min}, x_{max}]^2 = [-15, 15]^2$ remains unchanged and the total number of nodes N^2 is chosen as: $512^2, 1024^2, 2048^2, 4096^2$ and 8192^2 for each case. So, $\Delta x = \frac{x_{max}-x_{min}}{N}$ tends to be smaller as N becomes larger. The convergence of the option value at $(S_1, S_2) = (100, 100)$ is displayed in Table (4.19).

Nodes	Price	Change
512^2	8.44537854	
1024^2	8.43882006	0.00655847
2048^2	8.43248399	0.00633607
4096^2	8.43311492	-0.00063093
8192^2	8.43310941	0.00000551

Table 4.19: Convergence table of a European spread put under the shared-jump diffusion model using constant padding: *constant* Ω*, various* Δx

On the other hand, $\Delta x = 0.0073$ remains constant and the domain $\Omega = [x_{min}, x_{max}]^2$ is selected to be: $[-11, 11]^2, [-12, 12]^2, [-13, 13]^2, [-14, 14]^2$ and $[-15, 15]^2$ for each case. The convergence of the option value at $(S_1, S_2) = (100, 100)$ is displayed in Table (4.20).

Domain	Price	Change
$[-11, 11]^2$	8.43310421	
$[-12, 12]^2$	8.43311077	-0.00000655
$[-13, 13]^2$	8.43311310	-0.00000233
$[-14, 14]^2$	8.43311480	-0.00000171
$[-15, 15]^2$	8.43311492	-0.00000012

Table 4.20: Convergence table of a European spread put under the shared-jump diffusion model using constant padding: *constant* Δx*, various* Ω

Chapter 5

Empirical Data Analysis

5.1 Data Exploration

In order to justify the validity of the shared-jump diffusion model, the daily and monthly total return data of the following three main financial markets' index, S&P 500[1], Eurostox[2] and FTSE[3], were extracted from Thomson-Reuters Eikon[4]. All returns are from December 31, 1991 to December 31, 2017, including dividends and distributions.

In Figure (5.1), the same trend of prices can be observed for S&P 500, Eurostox and FTSE, especially when dramatic fluctuations happened. All the prices are rescaled to start from 1000 in USD, dating from December 31, 1991 to December 31, 2017.

From the plot of log returns Figure (5.2), S&P 500, Eurostox and FTSE tend to share almost the same fluctuations at same time, which reflects the contagion effects on global financial markets.

Figures (5.3), (5.4) and (5.5) compare the daily and monthly observed densities of log returns of S&P 500, Eurostox and FTSE with the standard normal density. Note that all the log returns are rescaled to zero mean, unit standard deviation. It is clear to see that there exist some improbable log returns compared with standard normal distribution. Hence, these cases can be determined as jumps rather than Brownian motion changes.

[1]S&P 500 is an American stock market index based on the market capitalizations of 500 large companies having common stock listed on the NYSE or NASDAQ.

[2]Eurostox is a stock index of fifty largest and most liquid Eurozone stocks.

[3]FTSE is a share index of the 100 companies listed on the London Stock Exchange with the highest market capitalization.

[4]Thomson-Reuters Eikon is a set of financial analysis tools. https://eikon.thomsonreuters.com/

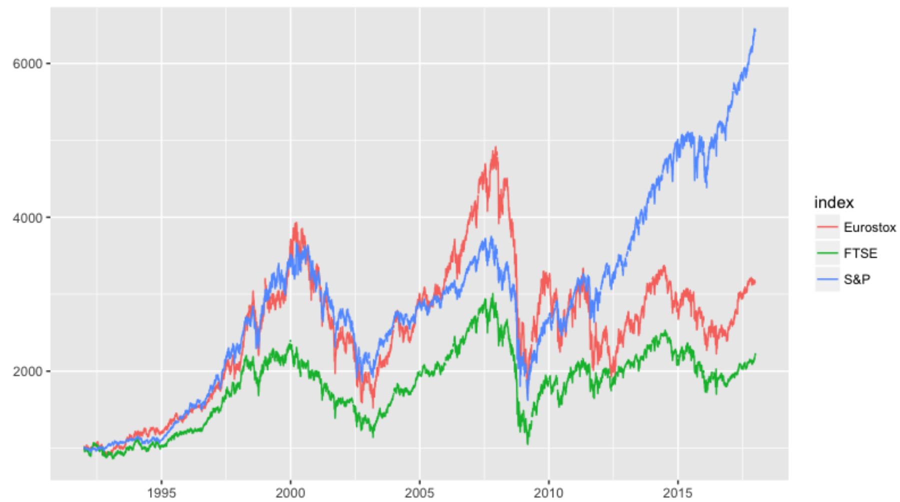

Figure 5.1: Prices of S&P 500, Eurostox and FTSE

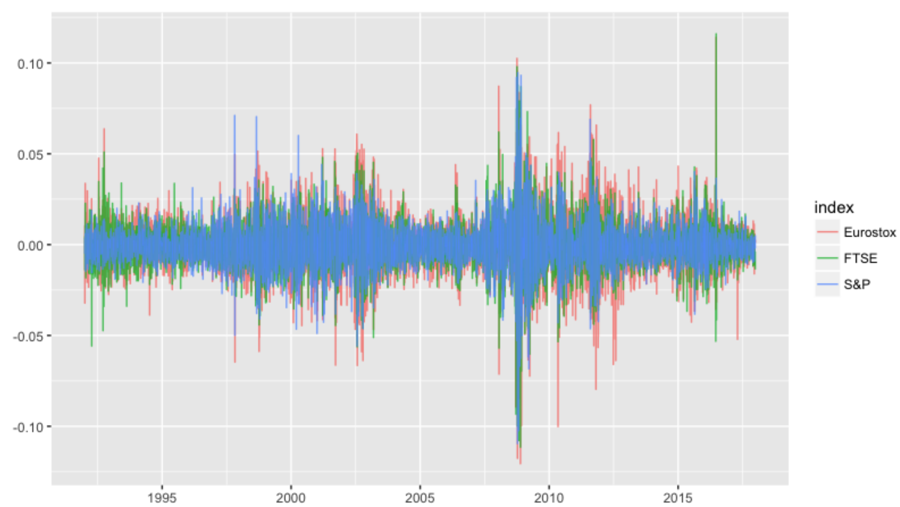

Figure 5.2: Log returns of S&P 500, Eurostox and FTSE

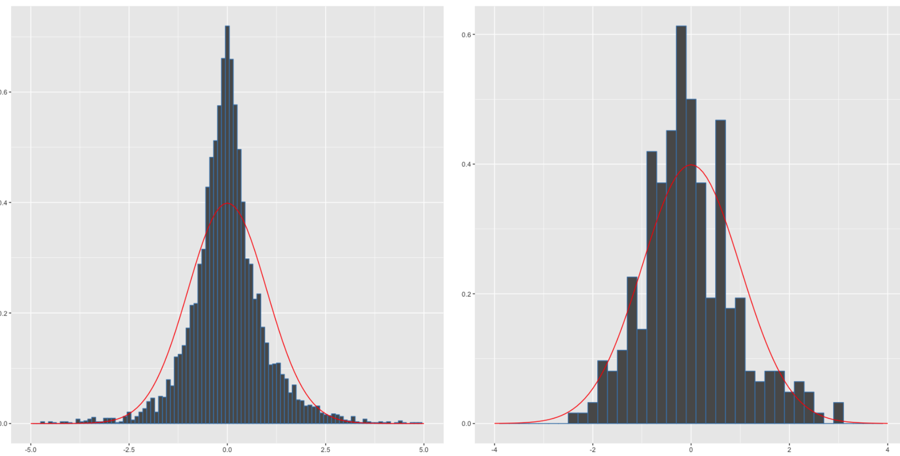

Figure 5.3: Scaled observed density and standard normal density of S&P 500 log returns.
Left: daily, Right: monthly

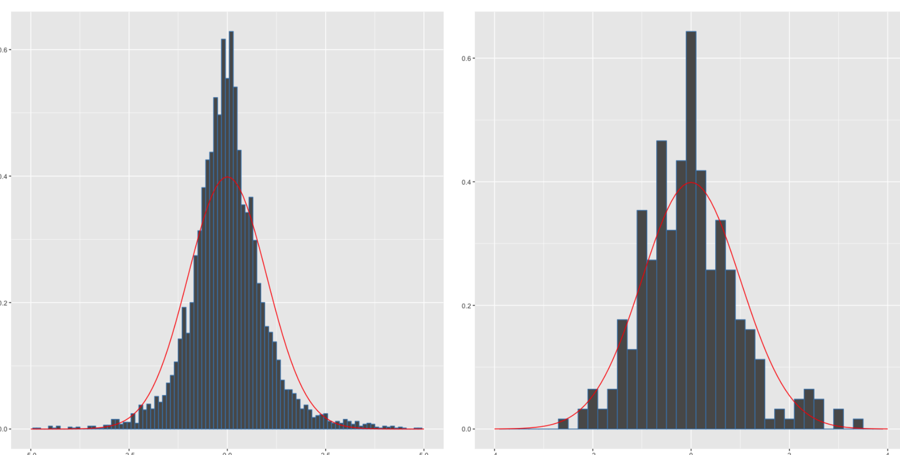

Figure 5.4: Scaled observed density and standard normal density of Eurostox log returns.
Left: daily, Right: monthly

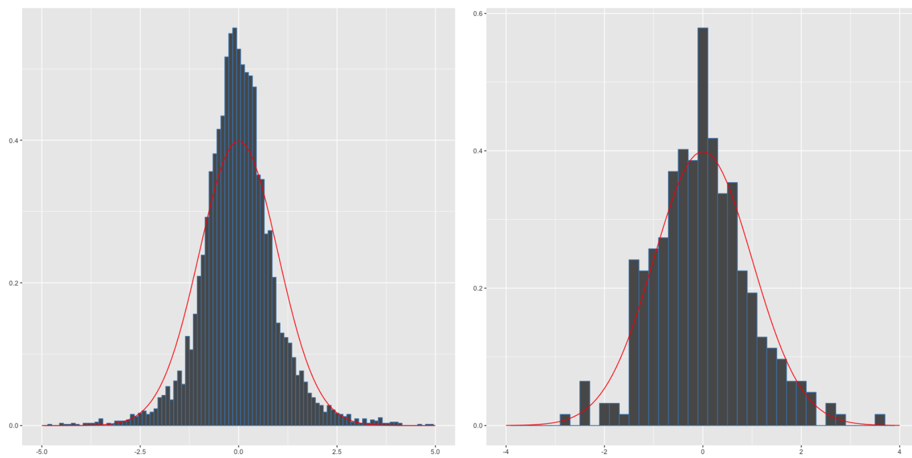

Figure 5.5: Scaled observed density and standard normal density of FTSE log returns. *Left: daily, Right: monthly*

Furthermore, the descriptive statistics for daily and monthly log returns of S&P 500, Eurostox and FTSE are displayed in Tables (5.1) and (5.2). The skewness tells that log returns follow the asymmetric distribution and kurtosis shows that higher frequency series tend to behave less like a normal distribution while lower frequency series behave more like a normal distribution.

Statistics	**S&P 500**	**Eurostox**	**FTSE**
Mean	-0.0003	-0.0001	-0.0001
Median	-0.0005	-0.0004	-0.0004
Stdev	0.0111	0.0148	0.0126
Skewness	0.2498	0.1397	0.2821
Kurtosis	9.4865	6.1047	8.2900

Table 5.1: Descriptive statistics for daily log returns of S&P 500, Eurostox and FTSE

Statistics	**S&P 500**	**Eurostox**	**FTSE**
Mean	-0.0060	-0.0037	-0.0026
Median	-0.0104	-0.0074	-0.0043
Stdev	0.0407	0.0593	0.0457
Skewness	0.8896	0.7558	0.5832
Kurtosis	2.1198	1.7267	1.8225

Table 5.2: Descriptive statistics for monthly log returns of S&P 500, Eurostox and FTSE

5.2 Empirical Estimates

With the intention of estimating appropriate parameters for the jump diffusion model, the daily and monthly total return series of the three indices from December 31, 1991 to December 31, 2017 are used. The methodology of parameter estimation is systematically mentioned in Dang and Forsyth (2016)[6] and Forsyth and Vetzal (2017)[7].

Consider discrete series of index prices $S(t_i) = S_i, i = 1, 2, \cdots, N+1$, with equal time intervals $\Delta t = t_{i+1} - t_i, \forall i$ and $T = N\Delta t$. Define the log returns ΔX_i as:

$$\Delta X_i = \log\left(\frac{S_{i+1}}{S_i}\right) \tag{5.1}$$

and the detrended log returns $\Delta \hat{X}_i$ as:

$$\begin{aligned} \Delta \hat{X}_i &= \Delta X_i - \hat{m}\Delta t \\ \hat{m} &= \frac{\log(S_{N+1}) - \log(S_1)}{T}. \end{aligned} \tag{5.2}$$

The important feature of a jump diffusion model is that it allows modelling of infrequent large jumps in underlying prices. The thresholding technique described by Mancini (2009)[13] is used to filter out the infrequent large jumps.

Suppose the estimate for the diffusive volatility component $\hat{\sigma}$ is given, then a jump can be detected by Shimizu (2013)[16] if

$$|\Delta \hat{X}_i| > \alpha \ \hat{\sigma} \ \frac{\sqrt{\Delta t}}{(\Delta t)^{\beta}} \tag{5.3}$$

where α and β are tuning parameters. The intuition behind equation (5.3) can be easily explained. For example, if $\alpha = 3$ and $\beta \ll 1$, then a return will be viewed as a jump if it is larger than a 3 standard deviation Brownian motion change, which would be improbable. Therefore, it should be considered as a jump.

Consequently, the jump detection indicators $\mathbf{1}_i^{up}$ and $\mathbf{1}_i^{dwn}$ are defined as follows:

$$\mathbf{1}_i^{up} = \begin{cases} 1, & \text{if } \Delta \hat{X}_i > \alpha\ \hat{\sigma}\sqrt{\Delta t} \\ 0, & \text{otherwise} \end{cases} \tag{5.4}$$

and

$$\mathbf{1}_i^{dwn} = \begin{cases} 1, & \text{if } \Delta \hat{X}_i < -\alpha\ \hat{\sigma}\sqrt{\Delta t} \\ 0, & \text{otherwise} \end{cases} . \tag{5.5}$$

Criteria (5.4) and (5.5) allows one to separate downward from upward jumps.

Define

$$\sum_{i=1}^{N} \mathbf{1}_i^{up} = N^{up};\ \sum_{i=1}^{N} \mathbf{1}_i^{dwn} = N^{dwn};\ N^{jmps} = N^{up} + N^{dwn};\ \sum_{i=1}^{N} \Big(1 - \mathbf{1}_i^{up} - \mathbf{1}_i^{dwn}\Big) = N^{gbm}$$

where N^{jmps} denotes the total number of jumps detected and N^{gbm} denotes the number of geometric Brownian motion increments. Then the estimate of the diffusive volatility is:

$$\hat{\sigma}^2 = \frac{1}{\Delta t}\ var\Big(\Big\{\Delta \hat{X}_i \mid \big(\mathbf{1}_i^{up} + \mathbf{1}_i^{dwn} = 0\big)\Big\}\Big). \tag{5.6}$$

Note that equations (5.4), (5.5) and (5.6) constitute an implicit equation for $\hat{\sigma}^2$, which must be solved by an iterative method by Clewlow and Strickland (2002)[5].

Given the estimate of the diffusive volatility $\hat{\sigma}^2$, other jump parameters can be estimated by:

$$\begin{aligned} \lambda &= \frac{N^{jmps}}{T}; & p &= \frac{N^{up}}{N^{jmps}}; \\ \eta_1 &= \frac{1}{mean\Big(\Big\{\Delta \hat{X}_i \mid (\mathbf{1}_i^{up} = 1)\Big\}\Big)}; & \eta_2 &= \frac{-1}{mean\Big(\Big\{\Delta \hat{X}_i \mid (\mathbf{1}_i^{dwn} = 1)\Big\}\Big)}. \end{aligned} \tag{5.7}$$

Once estimates for $\sigma, \lambda, p, \eta_1, \eta_2$ are fixed, the drift term is easy to be estimated as follows. From equation (2.1), let $X = log(S)$:

$$dX = \Big(\mu - \lambda\kappa - \frac{\sigma^2}{2}\Big)dt + \sigma dZ + \Big(\log(\eta)\Big)dq. \tag{5.8}$$

Taking expectations of both sides of (5.8) and assuming that only one jump takes place in $[t, t + dt]$ gives:

$$E[dX] = \Big(\mu - \lambda\kappa - \frac{\sigma^2}{2}\Big)dt + \lambda E[\log(\eta)]dt. \tag{5.9}$$

Recall $\kappa = E[\eta - 1]$. Writing equation (5.9) in discrete time leads to:

$$\frac{mean(\Delta X_i)}{\Delta t} = \Big(\mu - \lambda\kappa - \frac{\sigma^2}{2}\Big) + \lambda\Big(\frac{p}{\eta_1} - \frac{(1-p)}{\eta_2}\Big). \tag{5.10}$$

Therefore, given $\sigma, \lambda, p, \eta_1, \eta_2$, the drift term μ can be solved by equation (5.10).

The parameters estimated from real data are listed in Tables (5.3) and (5.4) :

Parameters	Value
α	5
T	26
N	6776
Δt	0.003837072

Parameters	**S&P 500**	**Eurostox**	**FTSE**
$\hat{m}$	0.071457034	0.04406454	0.030916764
$\hat{\sigma}$	0.165005933	0.225618585	0.189453899
N^{jmps}	25	20	19
N^{up}	10	10	6
λ	0.961538462	0.769230769	0.730769231
p	0.4	0.5	0.315789474
η_1	14.46086149	11.01653107	11.07519672
η_2	14.3162148	11.59146755	12.45671547
κ	-0.00945839	0.010208051	-0.019502028
μ	0.089985375	0.055513894	0.043757312

Table 5.3: Parameters estimated from daily data

Parameters	Value
α	3
T	26
N	312
Δt	0.083333333

Parameters	**S&P 500**	**Eurostox**	**FTSE**
$\hat{m}$	0.072230128	0.044368741	0.031416643
$\hat{\sigma}$	0.128230026	0.192026453	0.145231375
N^{jmps}	4	4	4
N^{up}	0	0	1
λ	0.153846154	0.153846154	0.153846154
p	0	0	0.25
η_1	-	-	7.822503629
η_2	6.663146548	4.843224528	5.840098476
κ	-	-	-0.073004105
μ	-	-	0.045071965

Table 5.4: Parameters estimated from monthly data

Note that for monthly data, there are no upward jumps detected by choosing $\alpha = 3$ for both S&P 500 and Eurostox. For details, the specific dates of jumps are shown in Table (5.5):

S&P 500	1998-08 $\downarrow$	2002-09 $\downarrow$	2008-10 $\downarrow$	2009-02 $\downarrow$
Eurostox	2002-07 $\downarrow$	2002-09 $\downarrow$	2008-10 $\downarrow$	2009-01 $\downarrow$
FTSE	2008-09 $\downarrow$	2008-10 $\downarrow$	2009-05 $\Uparrow$	2012-05 $\downarrow$

Table 5.5: Specific dates of jumps detected from monthly data

In the period of October 2008, which is known as the global financial crisis, all these three indices went through a huge downward jump. As for September 2002, both of S&P 500 and Eurostox suffered a big drop, which reflects the impact of the dot-com bubble. All the evidence here shows the significance of developing the shared-jump diffusion model.

Chapter 6

Conclusions

In this essay, a shared-jump diffusion model is developed to analyze financial shocks and contagion effects among global financial markets. The framework of options pricing under this new model by the Fourier Space Time-stepping (FST) method is presented. The FST method uses properties of the Fourier transform to convert the PIDE into a linear first-order ODE. As the numerical results shown, second order convergence is obtained by using the FST method under all three jump diffusion models. The option value solved by the FST method under the shared-jump diffusion model is consistent with Monte Carlo simulations, which reflects the accuracy and efficiency of the FST algorithm.

Furthermore, constant padding is introduced to remedy the wrap-around error for both of one- and two-dimensional option pricing cases. The methodology of expanding the original domain is elaborated in detail. Special treatment for the shared-jump diffusion model is also discussed. Stock index data in recent decades from US, Europe and Britain are gathered to conduct empirical data analysis. It can be shown that all three indices went through downward jumps during the dot-com bubble in 2002 and the global financial crisis in 2008.

As discussed in this essay, further research can include:

- Extending the FST method to price American and Asian options under the shared-jump diffusion model
- Developing more useful and efficient techniques to reduce the wrap-around error for single- and multi-asset cases
- Deriving a systematic framework for parameter estimation under the shared-jump diffusion model

APPENDICES

Appendix A

Fourier Transforms of Distributions

A.1 Fourier Transform of Normal Distribution

The density function of normal distribution can be written as

$$f(y) = \frac{1}{\sqrt{2\pi}\gamma} e^{-\frac{1}{2}(\frac{y-\mu}{\gamma})^2}.$$

So, the Fourier transform of $f(y)$ is defined as

$$F(k) := \int_{-\infty}^{\infty} \frac{1}{\sqrt{2\pi}\gamma} e^{-\frac{1}{2}(\frac{y-\mu}{\gamma})^2} \cdot e^{-2\pi iky} dy.$$

Let $x = y - \mu$, then $dx = dy$, so that

$$\begin{aligned} F(k) &= \int_{-\infty}^{\infty} \frac{1}{\sqrt{2\pi}\gamma} e^{-\frac{1}{2}(\frac{x}{\gamma})^2} \cdot e^{-2\pi ik(x+\mu)} dx \\ &= \frac{e^{-2\pi ik\mu}}{\sqrt{2\pi}\gamma} \int_{-\infty}^{\infty} e^{-\frac{1}{2}(\frac{x}{\gamma})^2} \cdot e^{-2\pi ikx} dx. \end{aligned}$$

By Euler's formula, $e^{-i\theta} = cos(\theta) - isin(\theta)$ gives

$$\begin{aligned} F(k) &= \frac{e^{-2\pi ik\mu}}{\sqrt{2\pi}\gamma} \int_{-\infty}^{\infty} e^{-\frac{1}{2}(\frac{x}{\gamma})^2} (cos(2\pi kx) - isin(2\pi kx)) dx \\ &= \frac{e^{-2\pi ik\mu}}{\sqrt{2\pi}\gamma} \Big(\int_{-\infty}^{\infty} e^{-\frac{1}{2}(\frac{x}{\gamma})^2} cos(2\pi kx) dx - i \int_{-\infty}^{\infty} e^{-\frac{1}{2}(\frac{x}{\gamma})^2} sin(2\pi kx) dx \Big). \end{aligned}$$

It is known that $sin(\theta)$ is an odd function while $cos(\theta)$ is an even function, so that $\int_{-\infty}^{\infty} e^{-\frac{1}{2}(\frac{x}{\gamma})^2} sin(2\pi kx)dx = 0$. Therefore, simplifying the equation above gives

$$F(k) = \frac{e^{-2\pi ik\mu}}{\sqrt{2\pi}\gamma} 2 \cdot \int_0^{\infty} e^{-\frac{1}{2}(\frac{x}{\gamma})^2} cos(2\pi kx)dx. \tag{A.1}$$

By the integral formula, $\int_0^{\infty} e^{-at^2} cos(2st)dt = \frac{1}{2}\sqrt{\frac{\pi}{a}} e^{\frac{-s^2}{a}}$, (A.1) can be expressed as

$$F(k) = \frac{e^{-2\pi ik\mu}}{\sqrt{2\pi}\gamma} 2 \cdot \int_0^{\infty} e^{-ax^2} cos(2sx)dx$$

where $a = \frac{1}{2\gamma^2}$ and $s = \pi k$. Using this formula obtains

$$\begin{aligned} F(k) &= \frac{e^{-2\pi ik\mu}}{\sqrt{2\pi}\gamma} 2\Big(\frac{1}{2}\sqrt{\frac{\pi}{a}} e^{\frac{-s^2}{a}}\Big) \\ &= \frac{e^{-2\pi ik\mu}}{\sqrt{2}\gamma} \sqrt{2\gamma^2} e^{-(\pi k)^2 2\gamma^2} \\ &= e^{-2\pi ik\mu} e^{-2(\pi k\gamma)^2} \\ &= e^{-2(\pi ik\mu + (\pi k\gamma)^2)}. \end{aligned}$$

Hence, $F(k) = e^{-2(\pi ik\mu + (\pi k\gamma)^2)}$ and $\bar{F}(k) = e^{2(\pi ik\mu - (\pi k\gamma)^2)}$.

A.2 Fourier Transform of Double Exponential Distribution

The density function of double exponential distribution is given by

$$f(y) = p\eta_1 e^{-y\eta_1} \cdot 1_{\{y\geq 0\}} + (1-p)\eta_2 e^{y\eta_2} \cdot 1_{\{y\leq 0\}}.$$

So, the Fourier transform of $f(y)$ is defined as

$$F(k) := \int_{-\infty}^{\infty} \Big(p\eta_1 e^{-y\eta_1} \cdot 1_{\{y\geq 0\}} + (1-p)\eta_2 e^{y\eta_2} \cdot 1_{\{y\leq 0\}} \Big) e^{-2\pi iky} dy.$$

It is easy to simplify the equation above as follows

$$\begin{aligned}
F(k) &= \int_{-\infty}^{\infty} p\eta_1 e^{-y\eta_1} \cdot 1_{\{y\geq 0\}} e^{-2\pi iky} + \int_{-\infty}^{\infty} (1-p)\eta_2 e^{y\eta_2} \cdot 1_{\{y\leq 0\}} e^{-2\pi iky} dy \\
&= \int_{0}^{\infty} p\eta_1 e^{-y\eta_1} \cdot e^{-2\pi iky} dy + \int_{-\infty}^{0} (1-p)\eta_2 e^{y\eta_2} \cdot e^{-2\pi iky} dy \\
&= p\eta_1 \int_{0}^{\infty} e^{-y(\eta_1+2\pi ik)} dy + (1-p)\eta_2 \int_{-\infty}^{0} e^{y(\eta_2-2\pi ik)} dy \\
&= p\eta_1 \Big[\frac{-1}{\eta_1+2\pi ik} e^{-y(\eta_1+2\pi ik)} \Big]_0^{\infty} + (1-p)\eta_2 \Big[\frac{1}{\eta_2-2\pi ik} e^{y(\eta_2-2\pi ik)} \Big]_{-\infty}^{0} \\
&= p\eta_1 \Big(\frac{1}{\eta_1+2\pi ik} \Big) + (1-p)\eta_2 \Big(\frac{1}{\eta_2-2\pi ik} \Big) \\
&= \frac{p}{1+2\pi ik(\frac{1}{\eta_1})} + \frac{1-p}{1-2\pi ik(\frac{1}{\eta_2})}.
\end{aligned}$$

Hence, $F(k) = \frac{p}{1+2\pi ik(\frac{1}{\eta_1})} + \frac{1-p}{1-2\pi ik(\frac{1}{\eta_2})}$ and $\bar{F}(k) = \frac{p}{1-2\pi ik(\frac{1}{\eta_1})} + \frac{1-p}{1+2\pi ik(\frac{1}{\eta_2})}$.

Appendix B

Algorithms for European Options

B.1 FST under One-factor Jump Diffusion Model

Data: $S, K, r, q, T, N, \sigma, \lambda, \mu, \gamma$
Result: V
$\mathbf{x} \leftarrow x_{min} + (0, 1, \cdots, N-1)\frac{x_{max}-x_{min}}{N}$;
$\mathbf{k} \leftarrow (0, 1, \cdots, \frac{N}{2}, -\frac{N}{2}+1, \cdots, -1)\frac{1}{(x_{max}-x_{min})}$;
$\mathbf{p} \leftarrow \max(Se^{\mathbf{x}} - K, 0)$(call); $\max(K - Se^{\mathbf{x}}, 0)$(put);
$\kappa \leftarrow e^{(\mu+\frac{1}{2}\gamma^2)} - 1$;
for $j \leftarrow 1$ **to** N **do**
$\quad \mathbf{\Psi}_j \leftarrow -\frac{\sigma^2}{2}(2\pi \mathbf{k}_j)^2 + (r - q - \lambda\kappa - \frac{\sigma^2}{2})(2\pi i \mathbf{k}_j) - (r + \lambda) + \lambda e^{2(\pi i \mathbf{k}_j \mu - (\pi \mathbf{k}_j \gamma)^2)}$
end
$\mathbf{v} \leftarrow \mathbf{p}$;
$\mathbf{v} \leftarrow IDFT[DFT[\mathbf{v}] \cdot e^{\mathbf{\Psi} T}]$;
$V \leftarrow$ interpolation of $\mathbf{v}$ at $x = 0$;

Algorithm 1: FST under One-factor Jump Diffusion Model: *Merton jump density*

Data: $S, K, r, q, T, N, \sigma, \lambda, p, \eta_1, \eta_2$
Result: V
$\mathbf{x} \leftarrow x_{min} + (0, 1, \cdots, N-1)\frac{x_{max}-x_{min}}{N}$;
$\mathbf{k} \leftarrow (0, 1, \cdots, \frac{N}{2}, -\frac{N}{2}+1, \cdots, -1)\frac{1}{(x_{max}-x_{min})}$;
$\mathbf{p} \leftarrow \max(Se^{\mathbf{x}} - K, 0)(\text{call});\ \max(K - Se^{\mathbf{x}}, 0)(\text{put})$;
$\kappa \leftarrow p\frac{\eta_1}{\eta_1-1} + (1-p)\frac{\eta_2}{\eta_2+1} - 1$;
for $j \leftarrow 1$ **to** N **do**
  $\mathbf{\Psi}_j \leftarrow -\frac{\sigma^2}{2}(2\pi\mathbf{k}_j)^2 + (r-q-\lambda\kappa-\frac{\sigma^2}{2})(2\pi i\mathbf{k}_j) - (r+\lambda) + \lambda\left(\frac{p}{1-2\pi i\mathbf{k}_j(\frac{1}{\eta_1})} + \frac{1-p}{1+2\pi i\mathbf{k}_j(\frac{1}{\eta_2})}\right)$
end
$\mathbf{v} \leftarrow \mathbf{p}$;
$\mathbf{v} \leftarrow IDFT[DFT[\mathbf{v}] \cdot e^{\mathbf{\Psi}T}]$;
$V \leftarrow$ interpolation of $\mathbf{v}$ at $x = 0$;
Algorithm 2: FST under One-factor Jump Diffusion Model: *Kou jump density*

B.2 FST under Two-factor Jump Diffusion Model

Data: $S, K, B_1, B_2, r, q_1, q_2, T, N, \sigma_1, \sigma_2, \rho, \lambda_1, \lambda_2, \mu_1, \mu_2, \gamma_1, \gamma_2$
Result: V
$\mathbf{x1}, \mathbf{x2} \leftarrow x_{min} + (0, 1, \cdots, N-1)\frac{x_{max}-x_{min}}{N}$;
$\mathbf{k1}, \mathbf{k2} \leftarrow (0, 1, \cdots, \frac{N}{2}, -\frac{N}{2}+1, \cdots, -1)\frac{1}{(x_{max}-x_{min})}$;
$\kappa_1 \leftarrow e^{(\mu_1+\frac{1}{2}\gamma_1^2)} - 1$;
$\kappa_2 \leftarrow e^{(\mu_2+\frac{1}{2}\gamma_2^2)} - 1$;
for $l \leftarrow 1$ **to** N **do**
  for $j \leftarrow 1$ **to** N **do**
    $\mathbf{p}_{lj} \leftarrow \max(B_2 S e^{\mathbf{x2}_j} - B_1 S e^{\mathbf{x1}_j} - K, 0)$ (spread call);
     $\max(K - B_2 S e^{\mathbf{x2}_j} + B_1 S e^{\mathbf{x1}_j}, 0)$ (spread put);
  end
end
for $l \leftarrow 1$ **to** N **do**
  for $j \leftarrow 1$ **to** N **do**
    $\mathbf{\Psi}_{lj} \leftarrow -\frac{\sigma_1^2}{2}(2\pi\mathbf{k1}_l)^2 - \frac{\sigma_2^2}{2}(2\pi\mathbf{k2}_j)^2 + (r - q_1 - \lambda_1\kappa_1 - \frac{\sigma_1^2}{2})(2\pi i\mathbf{k1}_l) + (r - q_2 - \lambda_2\kappa_2 - \frac{\sigma_1^2}{2})(2\pi i\mathbf{k2}_j) + \rho\sigma_1\sigma_2(2\pi\mathbf{k1}_l)(2\pi\mathbf{k2}_j) - (r + \lambda_1 + \lambda_2) + \lambda_1 e^{2(\pi i\mathbf{k1}_l\mu_1 - (\pi\mathbf{k1}_l\gamma_1)^2)} + \lambda_2 e^{2(\pi i\mathbf{k2}_j\mu_2 - (\pi\mathbf{k2}_j\gamma_2)^2)}$
  end
end
$\mathbf{v} \leftarrow \mathbf{p}$;
$\mathbf{v} \leftarrow IDFT[DFT[\mathbf{v}] \cdot e^{\mathbf{\Psi}T}]$;
$V \leftarrow$ interpolation of $\mathbf{v}$ at $x_1 = 0, x_2 = 0$;

Algorithm 3: FST under Two-factor Jump Diffusion Model: *Merton jump density*

B.3 FST under Shared-jump Diffusion Model

Data: $S, K, B_1, B_2, r, T, N, \sigma_1, \sigma_2, \rho, \lambda, p, \eta_1, \eta_2$
Result: V
$\mathbf{x1}, \mathbf{x2} \leftarrow x_{min} + (0, 1, \cdots, N-1)\frac{x_{max}-x_{min}}{N}$;
$\mathbf{k1}, \mathbf{k2} \leftarrow (0, 1, \cdots, \frac{N}{2}, -\frac{N}{2}+1, \cdots, -1)\frac{1}{(x_{max}-x_{min})}$;
$\kappa \leftarrow p\frac{\eta_1}{\eta_1-1} + (1-p)\frac{\eta_2}{\eta_2+1} - 1$;
for $l \leftarrow 1$ **to** N **do**
  for $j \leftarrow 1$ **to** N **do**
    $\mathbf{p}_{lj} \leftarrow \max(B_2 S e^{\mathbf{x2}_j} - B_1 S e^{\mathbf{x1}_j} - K, 0)$ (spread call);
     $\max(K - B_2 S e^{\mathbf{x2}_j} + B_1 S e^{\mathbf{x1}_j}, 0)$ (spread put);
  end
end
for $l \leftarrow 1$ **to** N **do**
  for $j \leftarrow 1$ **to** N **do**
    $\mathbf{\Psi}_{lj} \leftarrow$
     $-\frac{\sigma_1^2}{2}(2\pi\mathbf{k1}_l)^2 - \frac{\sigma_2^2}{2}(2\pi\mathbf{k2}_j)^2 + (r - \lambda\kappa - \frac{\sigma_1^2}{2})(2\pi i\mathbf{k1}_l) + (r - \lambda\kappa - \frac{\sigma_1^2}{2})(2\pi i\mathbf{k2}_j) +$
     $\rho\sigma_1\sigma_2(2\pi\mathbf{k1}_l)(2\pi\mathbf{k2}_j) - (r+\lambda) + \lambda\left(\frac{p}{1-2\pi i(\mathbf{k1}_l+\mathbf{k2}_j)(\frac{1}{\eta_1})} + \frac{1-p}{1+2\pi i(\mathbf{k1}_l+\mathbf{k2}_j)(\frac{1}{\eta_2})}\right)$
  end
end
$\mathbf{v} \leftarrow \mathbf{p}$;
$\mathbf{v} \leftarrow IDFT[DFT[\mathbf{v}] \cdot e^{\mathbf{\Psi}T}]$;
$V \leftarrow$ interpolation of $\mathbf{v}$ at $x_1 = 0, x_2 = 0$;
Algorithm 4: FST under Shared-jump Diffusion Model: *Kou jump density*

Appendix C

Monte Carlo Approach

C.1 Methodology

Consider the following stochastic differential equations (SDEs) in the risk neutral world:

$$\frac{dS_1}{S_1} = (r - \lambda^{\mathbb{Q}}\kappa^{\mathbb{Q}})dt + \sigma_1 dZ_1 + (\eta^{\mathbb{Q}} - 1)dq, \tag{C.1}$$

$$\frac{dS_2}{S_2} = (r - \lambda^{\mathbb{Q}}\kappa^{\mathbb{Q}})dt + \sigma_2 dZ_2 + (\eta^{\mathbb{Q}} - 1)dq, \tag{C.2}$$

$$dZ_1 dZ_2 = \rho dt \tag{C.3}$$

where $\lambda^{\mathbb{Q}}, \kappa^{\mathbb{Q}}$ and $\eta^{\mathbb{Q}}$ are all risk adjusted parameters under the $\mathbb{Q}$-measure.

After a log transformation $X_t = \log(S_t)$, equations (C.1) and (C.2) can be rewritten as:

$$dX_{1,t} = (r - \frac{\sigma_1^2}{2} - \lambda^{\mathbb{Q}}\kappa^{\mathbb{Q}})dt + \sigma_1 dZ_1 + \log(\eta_t^{\mathbb{Q}})dq, \tag{C.4}$$

$$dX_{2,t} = (r - \frac{\sigma_2^2}{2} - \lambda^{\mathbb{Q}}\kappa^{\mathbb{Q}})dt + \sigma_2 dZ_2 + \log(\eta_t^{\mathbb{Q}})dq \tag{C.5}$$

where

$$dq = \begin{cases} 0, & \text{with probability } 1 - \lambda^{\mathbb{Q}}dt, \\ 1, & \text{with probability } \lambda^{\mathbb{Q}}dt. \end{cases}$$

Under the shared-jump diffusion model, $\log(\eta^{\mathbb{Q}})$ follows a double exponential distribution. So, let $y = \log(\eta^{\mathbb{Q}})$, then the density of y, $f(y)$ is:

$$f(y) = p\eta_1 e^{-y\eta_1} \cdot 1_{\{y\geq 0\}} + (1-p)\eta_2 e^{y\eta_2} \cdot 1_{\{y\leq 0\}}.$$

Also, $\kappa^{\mathbb{Q}} = E[\eta^{\mathbb{Q}} - 1] = p\frac{\eta_1}{\eta_1 - 1} + (1-p)\frac{\eta_2}{\eta_2+1} - 1$. In addition, dq is assumed to be independent with $\eta_t^{\mathbb{Q}}$. The condition $\lambda^{\mathbb{Q}}\Delta t \ll 1$ guarantees that the probability of having more than one jump in $[t, t+\Delta t]$ is negligible.

Suppose no jump occurs in $[t, t+\Delta t]$, by forward Euler, the equations (C.4) and (C.5) give:

$$X_{1,t+\Delta t} = X_{1,t} + (r - \frac{\sigma_1^2}{2} - \lambda^{\mathbb{Q}}\kappa^{\mathbb{Q}})\Delta t + \sigma_1 \phi_{1,t}\sqrt{\Delta t}, \tag{C.6}$$

$$X_{2,t+\Delta t} = X_{2,t} + (r - \frac{\sigma_2^2}{2} - \lambda^{\mathbb{Q}}\kappa^{\mathbb{Q}})\Delta t + \sigma_2 \phi_{2,t}\sqrt{\Delta t} \tag{C.7}$$

where Δt is the finite timestep and $\phi_{1,t}$ and $\phi_{2,t}$ are two random numbers from standard normal distribution. The correlation between $\phi_{1,t}$ and $\phi_{2,t}$ is ρ. If there exists a jump in $[t, t+\Delta t]$, by forward Euler, the equations (C.4) and (C.5) give:

$$X_{1,t+\Delta t} = X_{1,t} + (r - \frac{\sigma_1^2}{2} - \lambda^{\mathbb{Q}}\kappa^{\mathbb{Q}})\Delta t + \sigma_1 \phi_{1,t}\sqrt{\Delta t} + y_t, \tag{C.8}$$

$$X_{2,t+\Delta t} = X_{2,t} + (r - \frac{\sigma_2^2}{2} - \lambda^{\mathbb{Q}}\kappa^{\mathbb{Q}})\Delta t + \sigma_2 \phi_{2,t}\sqrt{\Delta t} + y_t \tag{C.9}$$

where y_t is a random number from the double exponential distribution.

Therefore, the realized paths for S_1 and S_2 can be simulated using the method introduced above. After N timesteps, with $T = N\Delta t$, the option value can be derived given the payoff function: $V = Payoff(S_{1,T}, S_{2,T})$. Suppose the total number of trials is M and denote the payoff after the m^{th} trial as $Payoff(m)$, where $m = 1, \cdots, M$. So, the no-arbitrage value of the option is:

$$\begin{aligned} Value &= e^{-rT} E^{\mathbb{Q}}[Payoff] \\ &\approx e^{-rT} \frac{1}{M} \sum_{m=1}^{M} Payoff(m). \end{aligned} \tag{C.10}$$

Furthermore, the sampling error can be estimated via a statistical approach. With the estimated mean of the sample

$$\hat{\mu} = e^{-rT} \frac{1}{M} \sum_{m=1}^{M} Payoff(m) \tag{C.11}$$

and the standard deviation of the estimate

$$\omega = \sqrt{\frac{1}{M-1}\sum_{m=1}^{M}\left(e^{-rT}Payoff(m) - \hat{\mu}\right)^2}, \tag{C.12}$$

the 95% confidence interval for the actual value of the option V is:

$$\hat{\mu} - \frac{1.96\ \omega}{\sqrt{M}} \leq V \leq \hat{\mu} + \frac{1.96\ \omega}{\sqrt{M}}. \tag{C.13}$$

C.2 Algorithm for Monte Carlo Simulation

Data: $S, K, B_1, B_2, r, T, \sigma_1, \sigma_2, \rho, \lambda, p, \eta_1, \eta_2, N, M$
Result: V, sd
$\Delta t \leftarrow \frac{T}{N}$;
$\kappa \leftarrow p\frac{\eta_1}{\eta_1 - 1} + (1-p)\frac{\eta_2}{\eta_2+1} - 1$;
$\mathbf{R} \leftarrow \begin{bmatrix} 1 & \rho \\ \rho & 1 \end{bmatrix}$;
$\mathbf{X}_{1,old}, \mathbf{X}_{2,old} \leftarrow \log(S)$;
$\mathbf{L} \leftarrow$ **Cholesky Decomposition**$(\mathbf{R})$;
for $i \leftarrow 1$ **to** N **do**
  JumpCheck $\leftarrow$ (**rand**$(M,1) \leq \lambda\Delta t$);
  RandomDraw $\leftarrow$ **rand**$(M,1)$;
  JumpSize $\leftarrow$ (**RandomDraw** $\leq p$) $\cdot$ **exprnd**$(\frac{1}{\eta_1}, M, 1) -$ (**RandomDraw** $>$ p) $\cdot$ **exprnd**$(\frac{1}{\eta_2}, M, 1)$;
  JumpSize $\leftarrow$ **JumpSize** $\cdot$ **JumpCheck**;
  $\mathbf{\Phi} \leftarrow$ **randn**$(M,2)\mathbf{L}$;
  $\mathbf{X}_{1,new} \leftarrow \mathbf{X}_{1,old} + (r - \frac{\sigma_1^2}{2} - \lambda\kappa)\Delta t + \sigma_1\sqrt{\Delta t} \cdot \mathbf{\Phi}(:,1) +$ **JumpSize**;
  $\mathbf{X}_{1,old} \leftarrow \mathbf{X}_{1,new}$;
  $\mathbf{X}_{2,new} \leftarrow \mathbf{X}_{2,old} + (r - \frac{\sigma_2^2}{2} - \lambda\kappa)\Delta t + \sigma_2\sqrt{\Delta t} \cdot \mathbf{\Phi}(:,2) +$ **JumpSize**;
  $\mathbf{X}_{2,old} \leftarrow \mathbf{X}_{2,new}$;
end
$(\mathbf{S}_1, \mathbf{S}_2) \leftarrow (e^{\mathbf{X}_{1,new}}, e^{\mathbf{X}_{2,new}})$;
$V \leftarrow \mathbf{mean}\big(e^{-rT} \cdot Payoff(\mathbf{S}_1, \mathbf{S}_2, K, B_1, B_2)\big)$;
$sd \leftarrow \mathbf{std}\big(e^{-rT} \cdot Payoff(\mathbf{S}_1, \mathbf{S}_2, K, B_1, B_2)\big)$;

Algorithm 5: Monte Carlo under Shared-jump Diffusion Model: *Kou jump density*

References

[1] F. Allen and D. Gale, *Financial contagion*, Journal of Political Economy, 108 (2000), pp. 1–33.

[2] T. Baig and I. Goldfajn, *Financial market contagion in the Asian crisis*, SSRN Electronic Journal, (1999).

[3] F. Black and M. Scholes, *The pricing of options and corporate liabilities*, Journal of Political Economy, 81 (1973), pp. 637–654.

[4] P. P. Boyle, *Options: A Monte Carlo approach*, Journal of Financial Economics, 4 (1977), pp. 323–338.

[5] L. Clewlow and C. Strickland, *Energy derivatives: Pricing and risk management*, Lacima, 2000.

[6] D. M. Dang and P. A. Forsyth, *Better than pre-commitment mean-variance portfolio allocation strategies: A semi-self-financing Hamilton-Jacobi-Bellman equation approach*, European Journal of Operational Research, 250 (2016), pp. 827–841.

[7] P. A. Forsyth and K. R. Vetzal, *Dynamic mean variance asset allocation: Tests for robustness*, International Journal of Financial Engineering, 04 (2017), p. 1750021.

[8] K. Jackson, S. Jaimungal, and V. Surkov, *Fourier Space Time-stepping for option pricing with Lévy models*, The Journal of Computational Finance, 12 (2008), pp. 1–29.

[9] N. Kiyotaki and J. Moore, *Evil is the root of all money*, American Economic Review, 92 (2002), pp. 62–66.

[10] S. G. Kou, *A jump-diffusion model for option pricing*, Management Science, 48 (2002), pp. 1086–1101.

[11] J. Lippa, *A Fourier Space Time-stepping approach applied to problems in finance*, Master's thesis, University of Waterloo, 2013.

[12] F. A. Longstaff, *The subprime credit crisis and contagion in financial markets*, Journal of Financial Economics, 97 (2010), pp. 436–450.

[13] C. Mancini, *Non-parametric threshold estimation for models with stochastic diffusion coefficient and jumps*, Scandinavian Journal of Statistics, 36 (2009), pp. 270–296.

[14] R. C. Merton, *Option pricing when underlying stock returns are discontinuous*, Journal of Financial Economics, 3 (1976), pp. 125–144.

[15] V. Naik, *Option valuation and hedging strategies with jumps in the volatility of asset returns*, The Journal of Finance, 48 (1993), pp. 1969–1984.

[16] Y. Shimizu, ed., *Threshold estimation for stochastic differential equations with jumps*, Hong Kong, 2013, Proceedings of the 59th ISI World Statistics Conference.

[17] V. Surkov, *Option pricing using Fourier Space Time-stepping framework*, PhD thesis, University of Toronto, 2009.

[18] D. Vayanos, *Flight to quality, flight to liquidity, and the pricing of risk*, (2004).

[19] P. Wilmott, *Derivatives: the theory and practice of financial engineering*, John Wiley and Sons, 1999.